Available online at www.sciencedirect.com
ScienceDirect
Journal of Sound and Vibration 311 (2008) 160–183
JOURNAL OF SOUND AND VIBRATION
www.elsevier.com/locate/jsvi

Radiation clusters and the active control of sound transmission through symmetric structures into free space

Tsutomu Kaizuka*[,1], Nobuo Tanaka

Department of Aerospace Engineering, Tokyo Metropolitan University, 6-6 Asahigaoka, Hino city, Tokyo 191-0065 Japan

Received 24 January 2007; received in revised form 9 August 2007; accepted 26 August 2007
Available online 24 October 2007

Abstract

The purpose of this paper is attenuating harmonic sound transmission through symmetric structures into free space using error signals derived from structural vibration sensors. It is well known that structural modal functions of symmetric structures are clustered to an even function or an odd function and each of the clusters uncouples with the other cluster in the radiated acoustic field. This indicates that the clusters are orthogonal contributors, i.e., independent contributors, with respect to the radiated acoustic field. In this paper, the clusters are referred to as "radiation clusters" in contrast with radiation modes, which are conventional orthogonal contributors with respect to the radiated acoustic power. The active control of harmonic sound transmission through symmetric structures into free space based upon independently measuring and controlling the individual radiation clusters, termed "radiation cluster control", is proposed. The approach falls into a category of middle authority control (MAC), which is between low authority control (LAC): structural modal control and high authority control (HAC): radiation modal control, possessing the benefit of practicality similar to LAC, while providing high control performance and some flexibility of control gain assignment similar to HAC. Specific examples relating to radiation cluster control of a simply supported rectangular plate in an infinite baffle are given.

1. Introduction

The use of structural control sources to attenuate sound transmission through flexible structures into free space offers advantages over the use of more conventional acoustic sources, one of these being system compactness: surface mounted actuators are much less intrusive than bulky speaker/cabinet arrangements. However, the gains in system compactness are not necessarily realized in practice when microphones placed in the far field of a radiating structure are used to provide controller error signals to achieve global attenuation. As an alternative, surface mounted structural sensors have also been used as error sensors that can hold system compactness in practice. Though a reduction in the vibration of the structure is achieved, a reduction in the sound radiated from the structure does not necessarily follow [1,2]. Such a disproportionate relationship between vibration and sound is caused by nonorthogonality of elemental radiators or structural modes in the

*Corresponding author.
E-mail address: u6991501@cc.tmit.ac.jp (T. Kaizuka).
[1]Research Fellow of the Japan Society for the Promotion of Science.

0022-460X/$ - see front matter
doi:10.1016/j.jsv.2007.08.025

radiated acoustic field [3]. Conventional active vibration control based on elemental radiators or structural modes is categorized as low authority control (LAC) in this paper, because a reduction in the velocities of the elemental radiators or structural modes does not necessarily lead to a reduction in the radiated sound.

It has been shown that it is possible to describe quantities from the vibration of the structure, which are orthogonal with respect to the radiated acoustic power [4]. One can sense the orthogonal contributors, referred to as radiation modes, using structural error sensors, thus the sound transmission through the structure into free space is successfully reduced even though the error signals are derived from the vibration of the structure. The approach involves decomposing the surface vibration, usually via singular value decomposition, into a number of surface velocity distributions, which contribute independently to the radiated acoustic power. To carry out radiation modal control, two kinds of radiation modal filters, which can measure the amplitudes of the individual radiation modes have been proposed: elemental radiator-based approach [3,5–8]; and structural mode-based approach [9,10]. In the case of elemental radiator-based approach, the radiation modal filters consist of weighting addition of outputs from discrete sensors, which placed over the surface of the structure. The advantage of the approach is that the amplitudes of the individual radiation modes can be measured directly by the complex normal velocity information at the discrete sensor locations, therefore the knowledge of the structural modal functions is not required, while the disadvantage of the approach is that a large number of discrete sensors as well as the knowledge of the acoustic impedance between each pair of the discrete sensor locations are required. In the case of structural mode-based approach, the radiation modal filters consist of weighting addition of outputs from structural modal filters [11–13], which can measure the amplitudes of the individual structural modes. The structural modal filters are constructed of not only lumped parameter sensors (discrete sensors) but also distributed parameter sensors. The advantage of the approach is that a large number of lumped parameter sensors can be replaced by less number of distributed parameter sensors, while the disadvantage of the approach is that the knowledge of both the structural modal functions and the radiation resistance of each pair of the structural modes is required. Ultimately, although radiation modal control is categorized as high authority control (HAC) in this paper, where emphasis is placed on that a reduction in the velocities of the radiation modes leads to a reduction in the radiated sound, neither elemental radiator-based approach nor structural mode-based approach is easy to implement in practice.

Cancellation of the complex volume velocity of the structure has been proposed as a strategy for the active control of the sound transmission [14–21]. The complex volume velocity of the structure is a good estimate of the amplitude of the lowest-order radiation mode which at low nondimensional frequencies, i.e., frequencies for which the size of the structure is small compared with the acoustic wave length, accounts for the majority of the radiated acoustic power. Thus, volume velocity cancellation results in the significant reduction of the sound transmission for low nondimensional frequency excitation, whereas volume velocity cancellation results in the poor reduction of the sound transmission for high nondimensional frequency excitation, i.e., frequencies for which the size of the structure is large compared with the acoustic wave length. The advantage of the approach is that the complex volume velocity can be measured using a single distributed parameter sensor, which is used as an error sensor in a single-channel active control system for the sound transmission. Volume velocity cancellation is categorized as middle authority control (MAC) in this paper where emphasis is placed on arranging a compromise between feasibility similar to LAC and reasonability similar to HAC.

The authors focus here on the common knowledge that the structural modal functions of the symmetric structure such as a beam [22] and a rectangular plate [23] are clustered to an even function or an odd function, and each of the clusters uncouples with the other cluster in the radiated acoustic field. This implies that the clusters are the orthogonal contributors, i.e., independent contributors, with respect to the radiated acoustic field. In this paper, the clusters are referred to as ‘‘radiation clusters’’ in contrast with radiation modes. It should be noted that there is an essential difference between the radiation modes and the radiation clusters: the radiation modes are the orthogonal contributors with respect to the radiated acoustic power in units of mode; and the radiation clusters are the orthogonal contributors with respect to the radiated acoustic field in units of cluster. From a viewpoint of the orthogonality with respect to the radiated acoustic power, the radiation modes are superior to the radiation clusters. Namely, minimizing the amplitudes of the radiation modes guarantees the reduction of the sound transmission [3,9], while minimizing the amplitudes of the radiation clusters does not necessarily guarantee the reduction of the sound transmission because the structural modes within the individual radiation cluster couple to each other in the radiated acoustic field. However, the radiation clusters may be still reasonable as error criteria for the active control of the sound transmission, because at low nondimensional frequencies the radiation efficiency groupings of the radiation modes of some symmetric structures correspond to the radiation clusters [22–24]. The even radiation cluster is a combination of the structural modes associated with the volumetric component, while the odd radiation cluster is a combination of the structural modes associated with the nonvolumetric component, and thereby at low nondimensional frequencies the even radiation cluster has much higher radiation efficiency than the odd radiation cluster. This indicates that for low nondimensional frequency excitation the even radiation cluster should be preferentially minimized rather than the odd radiation cluster in order to reduce the sound transmission. In contrast, for high nondimensional frequency excitation both the even and odd radiation clusters should be minimized simultaneously. If one could selectively measure and control each of the radiation clusters without spillover between the radiation clusters, the sound transmission would be reduced reasonably. Such observations provide the physical background for the current work.

The primary objective of this paper is to develop the filters, which can measure the individual radiation clusters in a symmetric structure without observation spillover, and the actuators, which can excite the individual radiation clusters in a symmetric structure without control spillover. The advantage of the approach is that only discrete sensors and discrete actuators located at symmetric coordinate on the surface of the structure are required, while the knowledge of the structural modal functions, the acoustic impedance of each pair of the discrete sensor locations, and the radiation resistance of each pair of the structural modes is not required. Radiation cluster control may be categorized as MAC as is the case with volume velocity cancellation. Note that volume velocity cancellation using a uniform-force actuator [14] is interpreted as a special case of radiation cluster control with the error criterion being the even radiation cluster. Volume velocity cancellation measures and controls the even radiation cluster only, while radiation cluster control can parallel measure and control the even and odd radiation clusters. Hence, radiation cluster control is more flexible than volume velocity cancellation, though the configuration of radiation cluster control is less simple than that of volume velocity cancellation.

The second objective is to numerically investigate the validity of radiation cluster control for the sound transmission through a simply supported rectangular plate in an infinite baffle. The plate is chosen because of the symmetry of the structure and the simplicity of the geometry. In addition, the modal behavior and characteristics of the plate are well understood, thus allowing effort to be concentrated on understanding the physical mechanisms involved in the control of the sound transmission.

Section 2 begins by developing the general theory of the sound transmission through the structure into free space. In Section 2.1, the radiated acoustic field is derived in two formulations: one in terms of the complex normal velocities of the elemental radiators [3]; and the other in terms of the complex normal velocity amplitudes of the structural modes [3,9]. Throughout these formulations, the nonorthogonality of the elemental radiators and the structural modes in the radiated acoustic field are reviewed, and it is shown that conventional active vibration control based on neither the elemental radiator nor the structural modes is reasonable for controlling the sound transmission. In Section 2.2, the radiation modes are derived in above two formulations and the orthogonality of the radiation modes is reviewed, with the result that radiation modal control is reasonable for controlling the sound transmission. Moreover, the implementation of radiation modal control is discussed and the difficulties in constructing the radiation modal filters are pointed out. Section 2.3 specializes the theories of volume velocity cancellation. Much of the material presented in Sections 2.1–2.3 are not new (as is indicated by the references throughout). It is represented here, with outline derivations when appropriate, in order to provide a self-contained and unified account of the base theory of the control of the sound transmission through the structure into free space. Section 2.4 deals with the theories of the radiation clusters as well as radiation cluster control. Section 3 numerically verifies the effectiveness of radiation cluster control for the sound transmission through a simply supported rectangular plate in an infinite baffle by comparison with conventional active vibration control, radiation modal control, and volume velocity cancellation. Section 4 summarizes significant conclusions of the work.

In this paper, the radiation clusters are discussed in the scope of sound radiation in free space. On the other hand, in the authors' other paper [25], the radiation clusters are discussed in the scope of sound radiation in enclosed space.

2. General theory

2.1. Conventional active vibration control: low authority control

First, formulation for the radiated acoustic power with respect to the elemental radiators [3] is presented. It is assumed that a vibrating structure surface is divided into M elemental radiators. The time-averaged frequency-dependent acoustic power, $W(\omega)$, can be then written as

$$W(\omega) = \mathbf{v}^{\mathrm{H}}(\omega)\mathbf{R}(\omega)\mathbf{v}(\omega), \tag{1}$$

where ω is the angular frequency, the superscript H is the conjugate transpose, $\mathbf{R}(\omega)$ is the $(M \times M)$, real, symmetric, positive definite matrix, which is proportional to the real part of the acoustic impedance between each pair of the elemental radiators' center locations, and $\mathbf{v}(\omega)$ is the $(M \times 1)$ vector of the complex normal velocities of the elemental radiators, which is written as

$$\mathbf{v}(\omega) = \begin{bmatrix} v(\mathbf{r}_1, \omega) & \cdots & v(\mathbf{r}_m, \omega) & \cdots & v(\mathbf{r}_M, \omega) \end{bmatrix}^{\mathrm{T}} = \mathbf{\Psi}^{\mathrm{T}}\mathbf{a}(\omega), \tag{2}$$

where

$$\mathbf{\Psi} = \begin{bmatrix} \boldsymbol{\psi}(\mathbf{r}_1) & \cdots & \boldsymbol{\psi}(\mathbf{r}_m) & \cdots & \boldsymbol{\psi}(\mathbf{r}_M) \end{bmatrix} \tag{3}$$

and where $\mathbf{r}_m$ is the center location of the mth elemental radiator, the superscript T is the transpose, $\boldsymbol{\psi}(\mathbf{r}_m)$ is the $(N \times 1)$ vector of the structural modal functions, $\mathbf{a}(\omega)$ is the $(N \times 1)$ vector of the structural modal amplitudes, and N is the total number of the structural modes of interest. It should be noted that $\mathbf{R}(\omega)$ is not necessarily diagonal, which implies that the complex normal velocities of the elemental radiators are not the orthogonal contributors with respect to the radiated acoustic power. Therefore, minimizing the complex normal velocities of the individual elemental radiators will not necessarily reduce the radiated acoustic power.

Next, formulation for the radiated acoustic power with respect to the structural modes [3,9] is presented. Substituting Eq. (2) into Eq. (1) yields

$$W(\omega) = \mathbf{a}^{\mathrm{H}}(\omega)\mathbf{M}(\omega)\mathbf{a}(\omega), \tag{4}$$

where

$$\mathbf{M}(\omega) = \mathbf{\Psi}\mathbf{R}(\omega)\mathbf{\Psi}^{\mathrm{T}} \tag{5}$$

and where $\mathbf{M}(\omega)$ is the $(N \times N)$, real, symmetric, positive definite matrix, which is proportional to the radiation resistance between each pair of the structural modes. It should be noted that $\mathbf{M}(\omega)$ is not necessarily diagonal, which implies that the amplitudes of the structural modes are not the orthogonal contributors with respect to the radiated acoustic field. Therefore, minimizing the complex amplitudes of the individual structural modes will not necessarily reduce the radiated acoustic power.

We categorize conventional active vibration control with the error criteria being the squared complex normal velocities of the elemental radiators or the squared complex amplitudes of the structural modes as LAC where emphasis is placed on being unsure about the reduction of the sound transmission.

2.2. Radiation modal control: high authority control

First, formulation for the radiation modes with respect to the elemental radiators [3] is presented. The matrix, $\mathbf{R}(\omega)$, is real and symmetric. It thus has an eigenvalue/eigenvector decomposition, which can be written as

$$\mathbf{R}(\omega) = \mathbf{Q}^{\mathrm{T}}(\omega)\mathbf{\Lambda}(\omega)\mathbf{Q}(\omega) \tag{6}$$

in which $\mathbf{Q}(\omega)$ is the $(M' \times M)$ orthogonal matrix of the eigenvectors, and $\mathbf{\Lambda}(\omega)$ is the $(M' \times M')$ diagonal matrix of the eigenvalues which are all positive real numbers, since $\mathbf{R}(\omega)$ is positive definite. Substituting Eq. (6) into Eq. (1) yields

$$W(\omega) = \mathbf{y}^{\mathrm{H}}(\omega)\mathbf{\Lambda}(\omega)\mathbf{y}(\omega), \tag{7}$$

where

$$\mathbf{y}(\omega) = \mathbf{Q}(\omega)\mathbf{v}(\omega) \tag{8}$$

and where $\mathbf{y}(\omega)$ is the $(M' \times 1)$ vector of the radiation modal amplitudes in terms of the complex normal velocities of the elemental radiators.

Next, formulation for the radiation modes with respect to the structural modes [3,9] is presented. The matrix, $\mathbf{M}(\omega)$, is real and symmetric. It thus has an eigenvalue/eigenvector decomposition, which can be written as

$$\mathbf{M}(\omega) = \mathbf{P}^{\mathrm{T}}(\omega)\mathbf{\Omega}(\omega)\mathbf{P}(\omega) \tag{9}$$

in which $\mathbf{P}(\omega)$ is the $(N' \times N)$ orthogonal matrix of the eigenvectors, and $\mathbf{\Omega}(\omega)$ is the $(N' \times N')$ diagonal matrix of the eigenvalues which are all positive real numbers, since $\mathbf{M}(\omega)$ is positive definite. Substituting Eq. (9) into Eq. (4) yields

$$W(\omega) = \mathbf{b}^{\mathrm{H}}(\omega)\mathbf{\Omega}(\omega)\mathbf{b}(\omega), \tag{10}$$

where

$$\mathbf{b}(\omega) = \mathbf{P}(\omega)\mathbf{a}(\omega) \tag{11}$$

and where $\mathbf{b}(\omega)$ is the $(N' \times 1)$ vector of the radiation modal amplitudes in terms of the complex amplitudes of the structural modes.

Eqs. (7) and (10) demonstrate that the acoustic power contribution from any radiation mode is equal to the square of its amplitude multiplied by the associated eigenvalue. The radiation modes are therefore orthogonal contributors to the radiated acoustic power, and hence the radiated acoustic power is directly reduced by minimizing the amplitudes of any of the radiation modes. To realize an active controller with the error criteria being the squared complex amplitudes of the radiation modes, it is necessary to construct the radiation modal filters, which can measure the complex amplitudes of the individual radiation modes. It is clear from Eqs. (8) and (11) that the acoustic impedance of each pair of the elemental areas, the radiation resistances of each pair of the structural modes, and the structural modal functions are necessary to construct the radiation modal filters. Note that the acoustic impedances, radiation resistances, and structural modal functions may be difficult to obtain with accuracy, when the geometry of the structure is complicated or the structural modal density is high. Consequently, although radiation modal control is categorized as HAC where emphasis is placed on being sure about the reduction of the sound transmission, the implementation of it is not easy.

2.3. Volume velocity cancellation: middle authority control

Cancellation of the complex volume velocity of the structure has been proposed as a strategy for the active control of the sound transmission [14]. The complex volume velocity of the structure is a good estimate of the amplitude of the lowest-order radiation mode which at low nondimensional frequencies accounts for the majority of the radiated acoustic power, and can be measured in practice using a single distributed parameter sensor which is used as an error sensor in a single-channel active control system for controlling the sound transmission. Volume velocity cancellation is positioned as a part of MAC where emphasis is place on arranging a compromise between feasibility similar to LAC and reasonability similar to HAC. The complex volume velocity of the structure, $Q(\omega)$, is simply the sum of the complex velocities at each of the elemental radiators multiplied by the associated elemental area, and can be written as

$$Q(\omega) = \mathbf{q}\mathbf{v}(\omega), \tag{12}$$

where $\mathbf{q}$ is the $(1 \times M)$ vector of the elemental areas.

2.4. Radiation cluster control: middle authority control

At first, this section reformulates the common knowledge: the structural modes are clustered to an even function or an odd function when the structure is symmetric; and each of the clusters uncouples with the other cluster in the radiated acoustic field. This implies that the clusters are the orthogonal contributors with respect to the radiated acoustic field. Then, this section proposes the method for measuring and controlling the individual clusters without causing spillover between the clusters.

Fig. 1 shows a schematic illustration of an example of the symmetric structures along the x direction. One can then find the clusters of the structural modes: the cluster associated with an even function along the x direction (the even cluster); and the cluster associated with an odd function along the x direction (the odd cluster). Further, one can find the symmetric coordinates on the surface of the structure: $\mathbf{r}_{1,k} = (x_{1,k}, y_{1,k})$ is the coordinate in the range of $x \geqslant 0$; and $\mathbf{r}_{2,k} = (x_{2,k}, y_{2,k}) = (-x_{1,k}, y_{1,k})$ is the coordinate in the range of $x \leqslant 0$ where $x_{1,k}$ is assumed to be positive and the subscript $k = 1,2,3,\ldots,M/2$. Note that the number of the clusters and the number of the sets of the symmetric coordinates are defined as $2^1 = 2$, respectively. If the structure was symmetric along the x and y directions, the number of the clusters and the number of the sets of the symmetric coordinates would be $2^2 = 4$, respectively. And if the structure was symmetric along the x, y, and z directions, the number of the clusters and the number of the sets of the symmetric coordinates would be $2^3 = 8$, respectively. For simplicity, this paper deals with the symmetric structure along the x direction only as shown in Fig. 1. However, the following discussion may be expandable to any symmetric structure. The structural modal functions are clustered as

$$\boldsymbol{\psi}(\mathbf{r}_m) = \begin{bmatrix} \boldsymbol{\psi}_e(\mathbf{r}_m) \\ \boldsymbol{\psi}_o(\mathbf{r}_m) \end{bmatrix}, \tag{13}$$

where $\boldsymbol{\psi}_e(\mathbf{r}_m)$ is the $(N_e \times 1)$ vector of the even cluster, $\boldsymbol{\psi}_o(\mathbf{r}_m)$ is the $(N_o \times 1)$ vector of the odd cluster, and N_e is the number of the structural modes which belong to the even cluster, and N_o is the number of the structural modes which belong to the odd cluster. Note that the structural cluster $\boldsymbol{\psi}_e(\mathbf{r}_m)$ and $\boldsymbol{\psi}_o(\mathbf{r}_m)$ satisfy the following formulae:

$$\boldsymbol{\psi}_e(\mathbf{r}_{1,k}) = \boldsymbol{\psi}_e(\mathbf{r}_{2,k}), \tag{14a}$$

$$\boldsymbol{\psi}_o(\mathbf{r}_{1,k}) = -\boldsymbol{\psi}_o(\mathbf{r}_{2,k}). \tag{14b}$$

Eq. (3) is then rewritten in a cluster form as

$$\boldsymbol{\Psi} = \begin{bmatrix} \boldsymbol{\Psi}_{e,1} & \boldsymbol{\Psi}_{e,2} \\ \boldsymbol{\Psi}_{o,1} & \boldsymbol{\Psi}_{o,2} \end{bmatrix}, \tag{15}$$

where the $(N_e \times M/2)$ submatrix, $\boldsymbol{\Psi}_{e,1}$, the $(N_e \times M/2)$ submatrix, $\boldsymbol{\Psi}_{e,2}$, the $(N_o \times M/2)$ submatrix, $\boldsymbol{\Psi}_{o,1}$, and the $(N_o \times M/2)$ submatrix, $\boldsymbol{\Psi}_{o,2}$, are defined as follows:

$$\boldsymbol{\Psi}_{e,1} = \begin{bmatrix} \boldsymbol{\psi}_e(\mathbf{r}_{1,1}) & \cdots & \boldsymbol{\psi}_e(\mathbf{r}_{1,k}) & \cdots & \boldsymbol{\psi}_e(\mathbf{r}_{1,M/2}) \end{bmatrix}, \tag{16a}$$

$$\boldsymbol{\Psi}_{e,2} = \begin{bmatrix} \boldsymbol{\psi}_e(\mathbf{r}_{2,1}) & \cdots & \boldsymbol{\psi}_e(\mathbf{r}_{2,k}) & \cdots & \boldsymbol{\psi}_e(\mathbf{r}_{2,M/2}) \end{bmatrix}, \tag{16b}$$

$$\boldsymbol{\Psi}_{o,1} = \begin{bmatrix} \boldsymbol{\psi}_o(\mathbf{r}_{1,1}) & \cdots & \boldsymbol{\psi}_o(\mathbf{r}_{1,k}) & \cdots & \boldsymbol{\psi}_o(\mathbf{r}_{1,M/2}) \end{bmatrix}, \tag{16c}$$

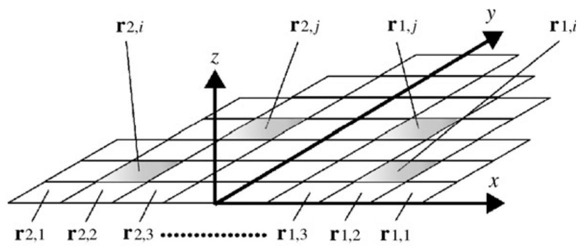

Fig. 1. An example of structures, which are symmetric along the x direction.

$$\mathbf{\Psi}_{o,2} = \begin{bmatrix} \boldsymbol{\psi}_o(\mathbf{r}_{2,1}) & \cdots & \boldsymbol{\psi}_o(\mathbf{r}_{2,k}) & \cdots & \boldsymbol{\psi}_o(\mathbf{r}_{2,M/2}) \end{bmatrix}. \tag{16d}$$

Following formulae are then satisfied:

$$\mathbf{\Psi}_{e,1} = \mathbf{\Psi}_{e,2}, \tag{17a}$$

$$\mathbf{\Psi}_{o,1} = -\mathbf{\Psi}_{o,2}. \tag{17b}$$

Considering Eqs. (1), (2) and (15), $\mathbf{R}(\omega)$ expands to

$$\mathbf{R}(\omega) = \begin{bmatrix} \mathbf{R}_{1,1}(\omega) & \mathbf{R}_{1,2}(\omega) \\ \mathbf{R}_{2,1}(\omega) & \mathbf{R}_{2,2}(\omega) \end{bmatrix}, \tag{18}$$

where the $(M/2 \times M/2)$ submatrix, $\mathbf{R}_{1,1}(\omega)$, the $(M/2 \times M/2)$ submatrix, $\mathbf{R}_{1,2}(\omega)$, the $(M/2 \times M/2)$ submatrix, $\mathbf{R}_{2,1}(\omega)$, and the $(M/2 \times M/2)$ submatrix, $\mathbf{R}_{2,2}(\omega)$ satisfy the following formulae:

$$\mathbf{R}_{1,1}(\omega) = \mathbf{R}_{2,2}(\omega), \tag{19a}$$

$$\mathbf{R}_{1,2}(\omega) = \mathbf{R}_{2,1}(\omega). \tag{19b}$$

Considering Eqs. (5), (15), (18), and (19), $\mathbf{M}(\omega)$ expands to

$$\mathbf{M}(\omega) = \begin{bmatrix} \mathbf{M}_e(\omega) & \mathbf{0} \\ \mathbf{0} & \mathbf{M}_o(\omega) \end{bmatrix}, \tag{20}$$

where the $(N_e \times N_e)$ submatrix, $\mathbf{M}_e(\omega)$, and the $(N_o \times N_o)$ submatrix, $\mathbf{M}_o(\omega)$, are defined as follows:

$$\mathbf{M}_e(\omega) = 2\mathbf{\Psi}_{e,1}\{\mathbf{R}_{1,1}(\omega) + \mathbf{R}_{1,2}(\omega)\}\mathbf{\Psi}_{e,1}^{\mathrm{T}}, \tag{21a}$$

$$\mathbf{M}_o(\omega) = 2\mathbf{\Psi}_{o,1}\{\mathbf{R}_{1,1}(\omega) - \mathbf{R}_{1,2}(\omega)\}\mathbf{\Psi}_{o,1}^{\mathrm{T}}. \tag{21b}$$

Eq. (20) implies the orthogonality of the clusters in the radiated acoustic field. Hence, the both clusters are regarded as the orthogonal contributors with respect to the radiated acoustic field, and referred to as ‘‘radiation clusters’’ in contrast with radiation modes. Substituting Eq. (20) into Eq. (4) gives an expression for the radiated acoustic power with respect to the radiation clusters

$$W(\omega) = W_e(\omega) + W_o(\omega), \tag{22}$$

where

$$W_e(\omega) = \mathbf{a}_e^{\mathrm{H}}(\omega)\mathbf{M}_{e,e}(\omega)\mathbf{a}_e(\omega), \tag{23a}$$

$$W_o(\omega) = \mathbf{a}_o^{\mathrm{H}}(\omega)\mathbf{M}_{o,o}(\omega)\mathbf{a}_o(\omega) \tag{23b}$$

and where $\mathbf{a}_e$ is the $(N_e \times 1)$ vectors of the even radiation cluster amplitudes and $\mathbf{a}_o$ are the $(N_o \times 1)$ vectors of the odd radiation cluster amplitudes (the vectors of the structural modal amplitudes in a cluster form). Eq. (22) implies that the radiated acoustic powers radiated from the even radiation cluster and the odd radiation clusters are independent to each other. Note that at low nondimensional frequencies the radiation efficiency groupings of the radiation modes of some symmetric structures correspond to the radiation clusters [22–24]: the radiation efficiency of the even radiation cluster is much higher than that of the odd radiation cluster. On the other hand, at high frequencies the radiation efficiencies of the radiation clusters are comparable to each other. This allows us to get the following insights for reducing the sound transmission: for low nondimensional frequency excitation the even radiation cluster should be preferentially minimized rather than the odd radiation cluster; and for high-frequency excitation both the even and odd radiation clusters should be minimized simultaneously.

We propose a novel active control approach referred to as ‘‘radiation cluster control’’ where emphasis is placed on controlling the individual radiation clusters without causing spillover between the radiation clusters. In what follows, we consider a simplistic system, a single input single output (SISO) arrangement based on feedforward control. Subsequently, we will expand the arrangement for multiple input multiple output

(MIMO) implementation. The number of the measurement points is assumed to be two, which is similar to the number of the radiation clusters. These two measurement points are located at the symmetric coordinates $\mathbf{r}_{1,i}$ and $\mathbf{r}_{2,i}$ (Fig. 1). Following formulae are then satisfied:

$$\boldsymbol{\psi}_e(\mathbf{r}_{1,i}) = \boldsymbol{\psi}_e(\mathbf{r}_{2,i}), \tag{24a}$$

$$\boldsymbol{\psi}_o(\mathbf{r}_{1,i}) = -\boldsymbol{\psi}_o(\mathbf{r}_{2,i}). \tag{24b}$$

The (2×1) vector of the complex normal velocities at the measurement points is given by

$$\begin{bmatrix} v(\mathbf{r}_{1,i}, \omega) \\ v(\mathbf{r}_{2,i}, \omega) \end{bmatrix} = \begin{bmatrix} \boldsymbol{\psi}_e^{\mathrm{T}}(\mathbf{r}_{1,i}) & \boldsymbol{\psi}_o^{\mathrm{T}}(\mathbf{r}_{1,i}) \\ \boldsymbol{\psi}_e^{\mathrm{T}}(\mathbf{r}_{2,i}) & \boldsymbol{\psi}_o^{\mathrm{T}}(\mathbf{r}_{2,i}) \end{bmatrix} \begin{bmatrix} \mathbf{a}_e(\omega) \\ \mathbf{a}_o(\omega) \end{bmatrix}. \tag{25}$$

Consider a simple arithmetic processing as

$$\begin{bmatrix} 1 & 1 \\ 1 & -1 \end{bmatrix} \begin{bmatrix} v(\mathbf{r}_{1,i}, \omega) \\ v(\mathbf{r}_{2,i}, \omega) \end{bmatrix} = \begin{bmatrix} v(\mathbf{r}_{1,i}, \omega) + v(\mathbf{r}_{2,i}, \omega) \\ v(\mathbf{r}_{1,i}, \omega) - v(\mathbf{r}_{2,i}, \omega) \end{bmatrix}, \tag{26}$$

where the row vectors of the coefficient matrix in Eq. (26), respectively, the (2×1) polar character vectors associated with in-phase and out-of-phase between the complex normal velocities at the symmetric measurement points as shown in Eq. (24). Substituting Eqs. (24) and (25) into Eq. (26) leads to

$$2\begin{bmatrix} \boldsymbol{\psi}_e^{\mathrm{T}}(\mathbf{r}_{1,i}) & \mathbf{0} \\ \mathbf{0} & \boldsymbol{\psi}_o^{\mathrm{T}}(\mathbf{r}_{1,i}) \end{bmatrix} \begin{bmatrix} \mathbf{a}_e(\omega) \\ \mathbf{a}_o(\omega) \end{bmatrix} = 2\begin{bmatrix} \boldsymbol{\psi}_e^{\mathrm{T}}(\mathbf{r}_{1,i})\mathbf{a}_e(\omega) \\ \boldsymbol{\psi}_o^{\mathrm{T}}(\mathbf{r}_{1,i})\mathbf{a}_o(\omega) \end{bmatrix} = \begin{bmatrix} v_e(\mathbf{r}_{1,i}, \omega) \\ v_o(\mathbf{r}_{1,i}, \omega) \end{bmatrix}. \tag{27}$$

Note that given values $v_e(\mathbf{r}_{1,i},\omega)$ and $v_o(\mathbf{r}_{1,i},\omega)$ are proportional to the complex normal velocities of the radiation clusters at the measurement point $\mathbf{r}_{1,i}$. The above filtering mechanisms for measuring the individual radiation clusters are referred to as "radiation cluster filters".

In the same manner as above filtering process, two point forces are located at the symmetric coordinates $\mathbf{r}_{1,j}$ and $\mathbf{r}_{2,j}$ (Fig. 1). Following formulae are then satisfied:

$$\boldsymbol{\psi}_e(\mathbf{r}_{1,j}) = \boldsymbol{\psi}_e(\mathbf{r}_{2,j}), \tag{28a}$$

$$\boldsymbol{\psi}_o(\mathbf{r}_{1,j}) = -\boldsymbol{\psi}_o(\mathbf{r}_{2,j}). \tag{28b}$$

The vector of the structural modal amplitudes, $\mathbf{a}(\omega)$, due to a distributed disturbance force, $f_d(\mathbf{r}, \omega)$, and a pair of the control forces at the symmetric coordinate, $f_1(\omega)$ and $f_2(\omega)$, is given by [1]

$$\mathbf{a}(\omega) = \mathbf{Y}(\omega)\left\{ \int_S \boldsymbol{\psi}(\mathbf{r}) f_d(\mathbf{r}, \omega)\,\mathrm{d}\mathbf{r} + \begin{bmatrix} \boldsymbol{\psi}(\mathbf{r}_{1,j}) & \boldsymbol{\psi}(\mathbf{r}_{1,j}) \end{bmatrix} \begin{bmatrix} f_1(\omega) \\ f_2(\omega) \end{bmatrix} \right\}, \tag{29}$$

where S is the surface of the structure, and $\mathbf{Y}(\omega)$ is the $(N \times N)$ diagonal structural resonance matrix whose diagonal terms are given by

$$Y_{nn}(\omega) = \frac{j\omega}{(\omega_n^2 - \omega^2 + j\eta_n\omega_n\omega)} \tag{30}$$

and where ω_n is the natural angular frequency of the nth structural mode, and η_n is the modal loss factor of the nth structural mode. Eq. (29) can be rewritten in a cluster form as

$$\mathbf{a}(\omega) = \begin{bmatrix} \mathbf{a}_e(\omega) \\ \mathbf{a}_o(\omega) \end{bmatrix} = \begin{bmatrix} \mathbf{Y}_e(\omega) & \mathbf{0} \\ \mathbf{0} & \mathbf{Y}_o(\omega) \end{bmatrix} \left\{ \begin{bmatrix} \int_S \boldsymbol{\psi}_e(\mathbf{r}) f_d(\mathbf{r}, \omega)\,\mathrm{d}\mathbf{r} \\ \int_S \boldsymbol{\psi}_o(\mathbf{r}) f_d(\mathbf{r}, \omega)\,\mathrm{d}\mathbf{r} \end{bmatrix} + \begin{bmatrix} \boldsymbol{\psi}_e(\mathbf{r}_{1,j}) & \boldsymbol{\psi}_e(\mathbf{r}_{2,j}) \\ \boldsymbol{\psi}_o(\mathbf{r}_{1,j}) & \boldsymbol{\psi}_o(\mathbf{r}_{2,j}) \end{bmatrix} \begin{bmatrix} f_1(\omega) \\ f_2(\omega) \end{bmatrix} \right\}. \tag{31}$$

At this point, consider a simple arithmetic processing as described for the radiation cluster filtering

$$\begin{bmatrix} 1 & 1 \\ 1 & -1 \end{bmatrix} \begin{bmatrix} f_1(\omega) \\ f_2(\omega) \end{bmatrix} = \begin{bmatrix} f_e(\omega) \\ f_o(\omega) \end{bmatrix}. \tag{32}$$

Substituting Eqs. (28) and (32) into Eq. (31) yields

$$\mathbf{a}(\omega) = \begin{bmatrix} \mathbf{a}_e(\omega) \\ \mathbf{a}_o(\omega) \end{bmatrix} = \begin{bmatrix} \mathbf{Y}_e(\omega)\{\int_S \boldsymbol{\psi}_e(\mathbf{r}) f_d(\mathbf{r},\omega)\,\mathrm{d}\mathbf{r} + \boldsymbol{\psi}_e(\mathbf{r}_{1,j}) f_e(\omega)\} \\ \mathbf{Y}_o(\omega)\{\int_S \boldsymbol{\psi}_o(\mathbf{r}) f_d(\mathbf{r},\omega)\,\mathrm{d}\mathbf{r} + \boldsymbol{\psi}_o(\mathbf{r}_{1,j}) f_o(\omega)\} \end{bmatrix}. \tag{33}$$

Note that control forces $f_e(\omega)$ and $f_o(\omega)$ obtained through the actuation process in Eq. (32) can control the even and odd radiation clusters, independently. The above mechanisms for actuating the individual radiation clusters are referred to as "radiation cluster actuators".

Finally, integrating the radiation cluster filters and actuators, a SISO arrangement of a radiation cluster control system can be described as

$$\begin{bmatrix} v_e(\mathbf{r}_{1,i},\omega) \\ v_o(\mathbf{r}_{1,i},\omega) \end{bmatrix} = 2\begin{bmatrix} \boldsymbol{\psi}_e(\mathbf{r}_{1,i})^{\mathrm{T}}\mathbf{Y}_e(\omega)\{\int_S \boldsymbol{\psi}_e(\mathbf{r}) f_d(\mathbf{r},\omega)\,\mathrm{d}\mathbf{r} + \boldsymbol{\psi}_e(\mathbf{r}_{1,j}) f_e(\mathbf{r}_{1,j},\omega)\} \\ \boldsymbol{\psi}_o(\mathbf{r}_{1,i})^{\mathrm{T}}\mathbf{Y}_o(\omega)\{\int_S \boldsymbol{\psi}_o(\mathbf{r}) f_d(\mathbf{r},\omega)\,\mathrm{d}\mathbf{r} + \boldsymbol{\psi}_o(\mathbf{r}_{1,j}) f_o(\mathbf{r}_{1,j},\omega)\} \end{bmatrix}. \tag{34}$$

Eq. (34) implies that there is no cross talk between the radiation cluster filtering sets $v_e(\mathbf{x}_{1,i},\omega)$ and $v_o(\mathbf{x}_{1,i},\omega)$, and the radiation cluster actuator sets $f_e(\omega)$ and $f_o(\omega)$; $f_e(\omega)$ and $f_o(\omega)$ are respectively transmitted to $v_e(\mathbf{x}_{1,i},\omega)$ and $v_o(\mathbf{x}_{1,i},\omega)$ without causing any spillover.

Furthermore, consider a MIMO arrangement of a radiation cluster control system which is constructed by I sets of the radiation cluster filters and J sets of the radiation cluster actuators. Eq. (34) is then expanded as

$$\begin{bmatrix} \mathbf{v}_e(\omega) \\ \mathbf{v}_o(\omega) \end{bmatrix} = \begin{bmatrix} \boldsymbol{\Psi}_{e,I}^{\mathrm{T}}\mathbf{Y}_e(\omega)\{\int_S \boldsymbol{\psi}_e(\mathbf{r}) f_d(\mathbf{r},\omega)\,\mathrm{d}\mathbf{r} + \boldsymbol{\Psi}_{e,J}\mathbf{f}_e(\omega)\} \\ \boldsymbol{\Psi}_{o,I}^{\mathrm{T}}\mathbf{Y}_o(\omega)\{\int_S \psi_o(\mathbf{r}) f_d(\mathbf{r},\omega)\,\mathrm{d}\mathbf{r} + \boldsymbol{\Psi}_{o,J}\mathbf{f}_o(\omega)\} \end{bmatrix} \tag{35}$$

where

$$\tilde{\mathbf{v}}_e(\omega) = \begin{bmatrix} v_e(\mathbf{r}_{1,1},\omega) & \cdots & v_e(\mathbf{r}_{1,i},\omega) & \cdots & v_e(\mathbf{r}_{1,I},\omega) \end{bmatrix}^{\mathrm{T}}, \tag{36a}$$

$$\tilde{\mathbf{v}}_o(\omega) = \begin{bmatrix} v_o(\mathbf{r}_{1,1},\omega) & \cdots & v_o(\mathbf{r}_{1,i},\omega) & \cdots & v_o(\mathbf{r}_{1,I},\omega) \end{bmatrix}^{\mathrm{T}}, \tag{36b}$$

$$\begin{bmatrix} v_e(\mathbf{r}_{1,i},\omega) \\ v_o(\mathbf{r}_{1,i},\omega) \end{bmatrix} = \begin{bmatrix} 1 & 1 \\ 1 & -1 \end{bmatrix}\begin{bmatrix} v(\mathbf{r}_{1,i},\omega) \\ v(\mathbf{r}_{2,i},\omega) \end{bmatrix} \quad (i = 1,2,\ldots,I), \tag{37}$$

$$\boldsymbol{\Psi}_{e,I} = 2\begin{bmatrix} \boldsymbol{\psi}_e(\mathbf{r}_{1,1}) & \cdots & \boldsymbol{\psi}_e(\mathbf{r}_{1,i}) & \cdots & \boldsymbol{\psi}_e(\mathbf{r}_{1,I}) \end{bmatrix}, \tag{38a}$$

$$\boldsymbol{\Psi}_{o,I} = 2\begin{bmatrix} \boldsymbol{\psi}_o(\mathbf{r}_{1,1}) & \cdots & \boldsymbol{\psi}_o(\mathbf{r}_{1,i}) & \cdots & \boldsymbol{\psi}_o(\mathbf{r}_{1,I}) \end{bmatrix}, \tag{38b}$$

$$\boldsymbol{\Psi}_{e,J} = \begin{bmatrix} \boldsymbol{\psi}_e(\mathbf{r}_{1,1}) & \cdots & \boldsymbol{\psi}_e(\mathbf{r}_{1,j}) & \cdots & \boldsymbol{\psi}_e(\mathbf{r}_{1,J}) \end{bmatrix}, \tag{39a}$$

$$\boldsymbol{\Psi}_{o,J} = \begin{bmatrix} \boldsymbol{\psi}_o(\mathbf{r}_{1,1}) & \cdots & \boldsymbol{\psi}_o(\mathbf{r}_{1,j}) & \cdots & \boldsymbol{\psi}_o(\mathbf{r}_{1,J}) \end{bmatrix}, \tag{39b}$$

$$\tilde{\mathbf{f}}_e(\omega) = \begin{bmatrix} f_{e,1}(\omega) & \cdots & f_{e,j}(\omega) & \cdots & f_{e,J}(\omega) \end{bmatrix}^{\mathrm{T}}, \tag{40a}$$

$$\tilde{\mathbf{f}}_o(\omega) = \begin{bmatrix} f_{o,1}(\omega) & \cdots & f_{o,j}(\omega) & \cdots & f_{o,J}(\omega) \end{bmatrix}^{\mathrm{T}}, \tag{40b}$$

$$\begin{bmatrix} f_{e,j}(\omega) \\ f_{o,j}(\omega) \end{bmatrix} = \begin{bmatrix} 1 & 1 \\ 1 & -1 \end{bmatrix}\begin{bmatrix} f_{1,j}(\omega) \\ f_{2,j}(\omega) \end{bmatrix} \quad (j = 1,2,\ldots,J) \tag{41}$$

and where $\mathbf{r}_{1,i}$ and $\mathbf{r}_{2,i}$ are the ith set of the symmetric measurement points, $\mathbf{r}_{1,j}$ and $\mathbf{r}_{2,j}$ are the jth set of the symmetric control points, and $f_{1,j}$ and $f_{2,j}$ are the jth set of point forces located at $\mathbf{r}_{1,j}$ and $\mathbf{r}_{2,j}$, respectively.

Consider the case when minimizing the sum of the squared complex normal velocities of the radiation clusters at the discrete measurement points by using the discrete point forces. From Eq. (35), the sum of the squared complex normal velocities of the radiation clusters at I measurement points is expressed as

$$\begin{bmatrix} \sum_{i=1}^{I} \left| v_e(\mathbf{r}_{1,i},\omega) \right|^2 \\ \sum_{i=1}^{I} \left| v_o(\mathbf{r}_{1,i},\omega) \right|^2 \end{bmatrix} = \begin{bmatrix} \tilde{\mathbf{v}}_e^{\mathrm{H}}(\omega)\tilde{\mathbf{v}}_e(\omega) \\ \tilde{\mathbf{v}}_o^{\mathrm{H}}(\omega)\tilde{\mathbf{v}}_o(\omega) \end{bmatrix}$$

$$= \begin{bmatrix} \tilde{\mathbf{f}}_e^{\mathrm{H}}(\omega)\mathbf{A}_e^{\mathrm{H}}(\omega)\mathbf{A}_e(\omega)\tilde{\mathbf{f}}_e(\omega) + \tilde{\mathbf{f}}_e^{\mathrm{H}}(\omega)\mathbf{A}_e^{\mathrm{H}}(\omega)\mathbf{b}_e(\omega) + \mathbf{b}_e(\omega)^{\mathrm{H}}\mathbf{A}_e(\omega)\tilde{\mathbf{f}}_e(\omega) + \mathbf{b}_e(\omega)^{\mathrm{H}}\mathbf{b}_e(\omega) \\ \tilde{\mathbf{f}}_o^{\mathrm{H}}(\omega)\mathbf{A}_o^{\mathrm{H}}(\omega)\mathbf{A}_o(\omega)\tilde{\mathbf{f}}_o(\omega) + \tilde{\mathbf{f}}_o^{\mathrm{H}}(\omega)\mathbf{A}_o^{\mathrm{H}}(\omega)\mathbf{b}_o(\omega) + \mathbf{b}_o(\omega)^{\mathrm{H}}\mathbf{A}_o(\omega)\tilde{\mathbf{f}}_o(\omega) + \mathbf{b}_o(\omega)^{\mathrm{H}}\mathbf{b}_o(\omega) \end{bmatrix} \tag{42}$$

where

$$\begin{bmatrix} \mathbf{A}_e(\omega) \\ \mathbf{A}_e(\omega) \end{bmatrix} = \begin{bmatrix} \mathbf{\Psi}_{e,I}^{\mathrm{T}}\mathbf{Y}_e(\omega)\mathbf{\Psi}_{e,J} \\ \mathbf{\Psi}_{o,I}^{\mathrm{T}}\mathbf{Y}_o(\omega)\mathbf{\Psi}_{o,J} \end{bmatrix}, \tag{43}$$

$$\begin{bmatrix} \mathbf{b}_e(\omega) \\ \mathbf{b}_o(\omega) \end{bmatrix} = \begin{bmatrix} \mathbf{\Psi}_{e,I}^{\mathrm{T}}\mathbf{Y}_e(\omega) \int_S \boldsymbol{\psi}_e(\mathbf{x}) f_d(\mathbf{x},\omega)\,\mathrm{d}\mathbf{x} \\ \mathbf{\Psi}_{o,I}^{\mathrm{T}}\mathbf{Y}_o(\omega) \int_S \boldsymbol{\psi}_o(\mathbf{x}) f_d(\mathbf{x},\omega)\,\mathrm{d}\mathbf{x} \end{bmatrix}. \tag{44}$$

Note that $\mathbf{A}_e(\omega)$ and $\mathbf{A}_o(\omega)$ are the transfer functions between the radiation cluster actuators and the radiation cluster filters, and $\mathbf{b}_e(\omega)$ and $\mathbf{b}_o(\omega)$ are the product of the disturbance force and the transfer functions between the disturbance force and the radiation cluster filters. Expressed in this form, the optimum set of the point forces, which produce the unique global minimum value of the quadratic function in Eq. (45), may be defined by the relationship [1]

$$\begin{bmatrix} \tilde{\mathbf{f}}_e(\omega) \\ \tilde{\mathbf{f}}_o(\omega) \end{bmatrix} = -\begin{bmatrix} \{\mathbf{A}_e^{\mathrm{H}}(\omega)\mathbf{A}_e(\omega)\}^{-1}\mathbf{A}_e^{\mathrm{H}}(\omega)\mathbf{b}_e(\omega) \\ \{\mathbf{A}_o^{\mathrm{H}}(\omega)\mathbf{A}_o(\omega)\}^{-1}\mathbf{A}_o^{\mathrm{H}}(\omega)\mathbf{b}_o(\omega) \end{bmatrix}. \tag{45}$$

Radiation cluster control may be a reasonable strategy for the active control of the sound transmission, because minimizing the sum of the squared complex normal velocities of the individual radiation clusters, which correspond to the radiation efficiency groupings of the radiation modes of some symmetric structures, is reasonable compared to minimizing the sum of the squared complex normal velocities of the elemental radiators or the sum of the squared complex amplitudes of the structural modes in a blind way, i.e., conventional active vibration control. However, minimizing the sum of the squared complex normal velocities of the individual radiation clusters does not necessarily guarantee the reduction of the radiated acoustic power, since the structural modes within the individual radiation cluster couple to each other in the radiated acoustic field ($\mathbf{M}_e(\omega)$ and $\mathbf{M}_o(\omega)$ are not generally diagonal matrixes). Although radiation cluster control provides a less direct way in controlling the sound transmission compared to radiation modal control, the configuration of radiation cluster control is much simpler than that of radiation modal control: radiation cluster control does not need the knowledge of the structural modal functions, the acoustic impedance of each pair of the discrete sensor locations, and the radiation resistance of each pair of the structural modes as is clear from Eq. (45). Moreover, volume velocity cancellation using a uniform-force actuator [14] may be interpreted as a special case of radiation cluster control with the error criterion being the even radiation cluster, because the arrangement of volume velocity cancellation fulfills a necessary condition for the radiation cluster filter and actuator with respect to the even radiation cluster. Volume velocity cancellation measures and controls the even radiation cluster only, whereas radiation cluster control can parallel measure and control the even and odd radiation clusters as seen in Eq. (42). Hence, radiation cluster control is more flexible than volume velocity cancellation, though the configuration of radiation cluster control is less simple than that of volume velocity cancellation. Consequently, radiation cluster control is categorized as a part of MAC.

3. Radiation cluster control of a rectangular plate

General theory of radiation cluster control in the previous section enables a prediction to be made of the optimum control forces, which will minimize the sum of the squared complex normal velocities of the radiation clusters. In the following section, the theoretical model will be specialized to a simply supported rectangular plate in an infinite baffle to be used later in the study of control mechanisms.

3.1. Specialization of general theory for the rectangular plate model case

The system of interest is a simply supported rectangular plate in an infinite baffle shown in Fig. 2. As mentioned in the previous section, the radiation clusters can be defined as the basis for even and odd functions into which the structural modal functions fall. The structural modal functions of a simply supported rectangular plate are [14]

$$\psi_n(\mathbf{r}_m) = \psi_{n_x/n_y}(x_m, y_m) = \sqrt{\frac{4}{L_x L_y}} \sin\frac{n_x \pi}{L_x} x_m \, \sin\frac{n_y \pi}{L_y} y_m, \quad n_x = 1, 2, 3, \ldots, N_x, \quad n_y = 1, 2, 3, \ldots, N_y, \tag{46}$$

where L_x and L_y are the dimensions of the plate, n_x and n_y are the structural modal indices, and N_x and N_y are the number of the structural modes of interest. The origin of the coordinate system is the leftmost corner of the plate shown in the figure. Considering even and odd function properties in the x and y directions, the radiation clusters are given by

$$\psi_{n_{e/e}}(\mathbf{r}_m) = \psi_{n_{x,o}/n_{y,o}}(x_m, y_m) = \sqrt{\frac{4}{L_x L_y}} \sin\frac{n_{x,o} \pi}{L_x} x_m \, \sin\frac{n_{y,o} \pi}{L_y} y_m \quad n_{x,o} = 1, 3, 5, \ldots N_{x,o}, \quad n_{y,o} = 1, 3, 5, \ldots N_{y,o}, \tag{47a}$$

$$\psi_{n_{e/o}}(\mathbf{r}_m) = \psi_{n_{x,o}/n_{y,e}}(x_m, y_m) = \sqrt{\frac{4}{L_x L_y}} \sin\frac{n_{x,o} \pi}{L_x} x_m \, \sin\frac{n_{y,e} \pi}{L_y} y_m \quad n_{x,o} = 1, 3, 5, \ldots N_{x,o}, \quad n_{y,e} = 2, 4, 6, \ldots N_{y,e}, \tag{47b}$$

$$\psi_{n_{o/e}}(\mathbf{r}_m) = \psi_{n_{x,e}/n_{y,o}}(x_m, y_m) = \sqrt{\frac{4}{L_x L_y}} \sin\frac{n_{x,e} \pi}{L_x} x_m \, \sin\frac{n_{y,o} \pi}{L_y} y_m \quad n_{x,e} = 2, 4, 6, \ldots N_{x,e}, \quad n_{y,o} = 1, 3, 5, \ldots N_{y,o}, \tag{47c}$$

$$\psi_{n_{o/o}}(\mathbf{r}_m) = \psi_{n_{x,e}/n_{y,e}}(x_m, y_m) = \sqrt{\frac{4}{L_x L_y}} \sin\frac{n_{x,e} \pi}{L_x} x_m \, \sin\frac{n_{y,e} \pi}{L_y} y_m \quad n_{x,e} = 2, 4, 6, \ldots N_{x,e}, \quad n_{y,e} = 2, 4, 6, \ldots N_{y,e}. \tag{47d}$$

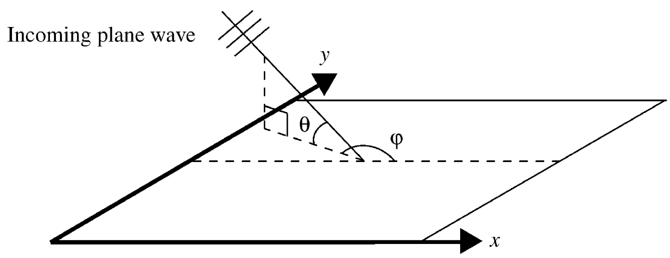

Fig. 2. A simply supported rectangular plate on which external plane wave is incident with the angles of elevation θ and azimuth φ.

The $(N \times 1)$ vector of the structural modal functions is then expressed as

$$\boldsymbol{\psi}(\mathbf{r}_m) = \begin{bmatrix} \boldsymbol{\psi}_{e/e}(\mathbf{r}_m) \\ \boldsymbol{\psi}_{e/o}(\mathbf{r}_m) \\ \boldsymbol{\psi}_{o/e}(\mathbf{r}_m) \\ \boldsymbol{\psi}_{o/o}(\mathbf{r}_m) \end{bmatrix}, \tag{48}$$

where

$$\psi_{e/e}(\mathbf{r}_m) = \begin{bmatrix} \psi_{1/1}(\mathbf{r}_m) & \cdots & \psi_{n_{x,o}/n_{y,o}}(\mathbf{r}_m) & \cdots & \psi_{N_{x,o}/N_{y,o}}(\mathbf{r}_m) \end{bmatrix}^{\mathrm{T}}, \tag{49a}$$

$$\psi_{e/o}(\mathbf{r}_m) = \begin{bmatrix} \psi_{1/2}(\mathbf{r}_m) & \cdots & \psi_{n_{x,o}/n_{y,e}}(\mathbf{r}_m) & \cdots & \psi_{N_{x,o}/N_{y,e}}(\mathbf{r}_m) \end{bmatrix}^{\mathrm{T}}, \tag{49b}$$

$$\psi_{o/e}(\mathbf{r}_m) = \begin{bmatrix} \psi_{2/1}(\mathbf{r}_m) & \cdots & \psi_{n_{x,e}/n_{y,o}}(\mathbf{r}_m) & \cdots & \psi_{N_{x,e}/N_{y,o}}(\mathbf{r}_m) \end{bmatrix}^{\mathrm{T}}, \tag{49c}$$

$$\psi_{o/o}(\mathbf{r}_m) = \begin{bmatrix} \psi_{2/2}(\mathbf{r}_m) & \cdots & \psi_{n_{x,e}/n_{y,e}}(\mathbf{r}_m) & \cdots & \psi_{N_{x,e}/N_{y,e}}(\mathbf{r}_m) \end{bmatrix}^{\mathrm{T}} \tag{49d}$$

and where $\boldsymbol{\psi}_{e/e}(\mathbf{r}_m)$ is the $(N_{e/e} \times 1)$ vector of the even/even radiation cluster defined in Eq. (47a), $\boldsymbol{\psi}_{\mathrm{e/o}}(\mathbf{r}_m)$ is the $(N_{e/o} \times 1)$ vector of the even/odd radiation cluster defined in Eq. (47b), $\boldsymbol{\psi}_{\mathrm{o/e}}(\mathbf{r}_m)$ is the $(N_{o/e} \times 1)$ vector of the odd/even radiation cluster defined in Eq. (47c), and $\boldsymbol{\psi}_{o/o}(\mathbf{r}_m)$ is the $(N_{o/o} \times 1)$ vector of the odd/odd radiation cluster defined in Eq. (47d). Radiation cluster control system is then described as

$$\begin{bmatrix} \sum_{i=1}^{I} |v_{e/e}(\mathbf{r}_{1,i},\omega)|^2 \\ \sum_{i=1}^{I} |v_{e/o}(\mathbf{r}_{1,i},\omega)|^2 \\ \sum_{i=1}^{I} |v_{o/e}(\mathbf{r}_{1,i},\omega)|^2 \\ \sum_{i=1}^{I} |v_{o/o}(\mathbf{r}_{1,i},\omega)|^2 \end{bmatrix} = \begin{bmatrix} \tilde{\mathbf{v}}^{\mathrm{H}}_{e/e}(\omega)\tilde{\mathbf{v}}_{e/e}(\omega) \\ \tilde{\mathbf{v}}^{\mathrm{H}}_{e/o}(\omega)\tilde{\mathbf{v}}_{e/o}(\omega) \\ \tilde{\mathbf{v}}^{\mathrm{H}}_{o/e}(\omega)\tilde{\mathbf{v}}_{o/e}(\omega) \\ \tilde{\mathbf{v}}^{\mathrm{H}}_{o/o}(\omega)\tilde{\mathbf{v}}_{o/o}(\omega) \end{bmatrix}$$

$$= \begin{bmatrix} \tilde{\mathbf{f}}^{\mathrm{H}}_{e/e}(\omega)\mathbf{A}^{\mathrm{H}}_{e/e}(\omega)\mathbf{A}_{e/e}(\omega)\tilde{\mathbf{f}}_{e/e}(\omega) + \tilde{\mathbf{f}}^{\mathrm{H}}_{e/e}(\omega)\mathbf{A}^{\mathrm{H}}_{e/e}(\omega)\mathbf{b}_{e/e}(\omega) + \mathbf{b}^{\mathrm{H}}_{e/e}(\omega)\mathbf{A}_{e/e}(\omega)\tilde{\mathbf{f}}_{e/e}(\omega) + \mathbf{b}^{\mathrm{H}}_{e/e}(\omega)\mathbf{b}_{e/e}(\omega) \\ \tilde{\mathbf{f}}^{\mathrm{H}}_{e/o}(\omega)\mathbf{A}^{\mathrm{H}}_{e/o}(\omega)\mathbf{A}_{e/o}(\omega)\tilde{\mathbf{f}}_{e/o}(\omega) + \tilde{\mathbf{f}}^{\mathrm{H}}_{e/o}(\omega)\mathbf{A}^{\mathrm{H}}_{e/o}(\omega)\mathbf{b}_{e/o}(\omega) + \mathbf{b}^{\mathrm{H}}_{e/o}(\omega)\mathbf{A}_{e/o}(\omega)\tilde{\mathbf{f}}_{e/o}(\omega) + \mathbf{b}^{\mathrm{H}}_{e/o}(\omega)\mathbf{b}_{e/o}(\omega) \\ \tilde{\mathbf{f}}^{\mathrm{H}}_{o/e}(\omega)\mathbf{A}^{\mathrm{H}}_{o/e}(\omega)\mathbf{A}_{o/e}(\omega)\tilde{\mathbf{f}}_{o/e}(\omega) + \tilde{\mathbf{f}}^{\mathrm{H}}_{o/e}(\omega)\mathbf{A}^{\mathrm{H}}_{o/e}(\omega)\mathbf{b}_{o/e}(\omega) + \mathbf{b}^{\mathrm{H}}_{o/e}(\omega)\mathbf{A}_{o/e}(\omega)\tilde{\mathbf{f}}_{o/e}(\omega) + \mathbf{b}^{\mathrm{H}}_{o/e}(\omega)\mathbf{b}_{o/e}(\omega) \\ \tilde{\mathbf{f}}^{\mathrm{H}}_{o/o}(\omega)\mathbf{A}^{\mathrm{H}}_{o/o}(\omega)\mathbf{A}_{o/o}(\omega)\tilde{\mathbf{f}}_{o/o}(\omega) + \tilde{\mathbf{f}}^{\mathrm{H}}_{o/o}(\omega)\mathbf{A}^{\mathrm{H}}_{o/o}(\omega)\mathbf{b}_{o/o}(\omega) + \mathbf{b}^{\mathrm{H}}_{o/o}(\omega)\mathbf{A}_{o/o}(\omega)\tilde{\mathbf{f}}_{o/o}(\omega) + \mathbf{b}^{\mathrm{H}}_{o/o}(\omega)\mathbf{b}_{o/o}(\omega) \end{bmatrix} \tag{50}$$

where

$$\tilde{\mathbf{v}}_{e/e}(\omega) = \begin{bmatrix} v_{e/e}(\mathbf{r}_{1,1},\omega) & \cdots & v_{e/e}(\mathbf{r}_{1,1},\omega) & \cdots & v_{e/e}(\mathbf{r}_{1,1},\omega) \end{bmatrix}^{\mathrm{T}}, \tag{51a}$$

$$\tilde{\mathbf{v}}_{e/o}(\omega) = \begin{bmatrix} v_{e/o}(\mathbf{r}_{1,1},\omega) & \cdots & v_{e/o}(\mathbf{r}_{1,i},\omega) & \cdots & v_{e/o}(\mathbf{r}_{1,I},\omega) \end{bmatrix}^{\mathrm{T}}, \tag{51b}$$

$$\tilde{\mathbf{v}}_{o/e}(\omega) = \begin{bmatrix} v_{o/e}(\mathbf{r}_{1,1},\omega) & \cdots & v_{o/e}(\mathbf{r}_{1,i},\omega) & \cdots & v_{o/e}(\mathbf{r}_{1,I},\omega) \end{bmatrix}^{\mathrm{T}}, \tag{51c}$$

$$\tilde{\mathbf{v}}_{o/o}(\omega) = \begin{bmatrix} v_{o/o}(\mathbf{r}_{1,1},\omega) & \cdots & v_{o/o}(\mathbf{r}_{1,i},\omega) & \cdots & v_{o/o}(\mathbf{r}_{1,I},\omega) \end{bmatrix}^{\mathrm{T}}, \tag{51d}$$

$$\begin{bmatrix} v_{e/e}(\mathbf{r}_{1,i},\omega) \\ v_{e/o}(\mathbf{r}_{1,i},\omega) \\ v_{o/e}(\mathbf{r}_{1,i},\omega) \\ v_{o/o}(\mathbf{r}_{1,i},\omega) \end{bmatrix} = \begin{bmatrix} +1 & +1 & +1 & +1 \\ +1 & +1 & -1 & -1 \\ +1 & -1 & -1 & +1 \\ +1 & -1 & +1 & -1 \end{bmatrix} \begin{bmatrix} v(\mathbf{r}_{1,i},\omega) \\ v(\mathbf{r}_{2,i},\omega) \\ v(\mathbf{r}_{3,i},\omega) \\ v(\mathbf{r}_{4,i},\omega) \end{bmatrix} \quad (i = 1, 2, \ldots, I), \tag{52}$$

$$\begin{bmatrix} \mathbf{A}_{e/e}(\omega) \\ \mathbf{A}_{e/o}(\omega) \\ \mathbf{A}_{o/e}(\omega) \\ \mathbf{A}_{o/o}(\omega) \end{bmatrix} = \begin{bmatrix} \mathbf{\Psi}^{\mathrm{T}}_{e/e,I}\mathbf{Y}_{e/e}(\omega)\mathbf{\Psi}_{e/e,J} \\ \mathbf{\Psi}^{\mathrm{T}}_{e/o,I}\mathbf{Y}_{e/o}(\omega)\mathbf{\Psi}_{e/o,J} \\ \mathbf{\Psi}^{\mathrm{T}}_{o/e,I}\mathbf{Y}_{o/e}(\omega)\mathbf{\Psi}_{o/e,J} \\ \mathbf{\Psi}^{\mathrm{T}}_{o/o,I}\mathbf{Y}_{o/o}(\omega)\mathbf{\Psi}_{o/o,J} \end{bmatrix}, \tag{53}$$

$$\begin{bmatrix} \mathbf{b}_{e/e}(\omega) \\ \mathbf{b}_{e/o}(\omega) \\ \mathbf{b}_{o/e}(\omega) \\ \mathbf{b}_{o/o}(\omega) \end{bmatrix} = \begin{bmatrix} \mathbf{\Psi}^{\mathrm{T}}_{e/e,I}\mathbf{Y}_{e/e}(\omega)\int_S \boldsymbol{\psi}_{e/e}(\mathbf{r}) f_d(\mathbf{r},\omega)\,\mathrm{d}\mathbf{r} \\ \mathbf{\Psi}^{\mathrm{T}}_{e/o,I}\mathbf{Y}_{e/o}(\omega)\int_S \boldsymbol{\psi}_{e/o}(\mathbf{r}) f_d(\mathbf{r},\omega)\,\mathrm{d}\mathbf{r} \\ \mathbf{\Psi}^{\mathrm{T}}_{o/e,I}\mathbf{Y}_{o/e}(\omega)\int_S \boldsymbol{\psi}_{o/e}(\mathbf{r}) f_d(\mathbf{r},\omega)\,\mathrm{d}\mathbf{r} \\ \mathbf{\Psi}^{\mathrm{T}}_{o/o,I}\mathbf{Y}_{o/o}(\omega)\int_S \boldsymbol{\psi}_{o/o}(\mathbf{r}) f_d(\mathbf{r},\omega)\,\mathrm{d}\mathbf{r} \end{bmatrix}, \tag{54}$$

$$\mathbf{\Psi}_{e/e,I} = \begin{bmatrix} \boldsymbol{\psi}_{e/e}(\mathbf{r}_{1,1}) & \cdots & \boldsymbol{\psi}_{e/e}(\mathbf{r}_{1,i}) & \cdots & \boldsymbol{\psi}_{e/e}(\mathbf{r}_{1,I}) \end{bmatrix}, \tag{55a}$$

$$\mathbf{\Psi}_{e/o,I} = \begin{bmatrix} \boldsymbol{\psi}_{e/o}(\mathbf{r}_{1,1}) & \cdots & \boldsymbol{\psi}_{e/o}(\mathbf{r}_{1,i}) & \cdots & \boldsymbol{\psi}_{e/o}(\mathbf{r}_{1,I}) \end{bmatrix}, \tag{55b}$$

$$\mathbf{\Psi}_{o/e,I} = \begin{bmatrix} \boldsymbol{\psi}_{o/e}(\mathbf{r}_{1,1}) & \cdots & \boldsymbol{\psi}_{o/e}(\mathbf{r}_{1,i}) & \cdots & \boldsymbol{\psi}_{o/e}(\mathbf{r}_{1,I}) \end{bmatrix}, \tag{55c}$$

$$\mathbf{\Psi}_{o/o,I} = \begin{bmatrix} \boldsymbol{\psi}_{o/o}(\mathbf{r}_{1,1}) & \cdots & \boldsymbol{\psi}_{o/o}(\mathbf{r}_{1,i}) & \cdots & \boldsymbol{\psi}_{o/o}(\mathbf{r}_{1,I}) \end{bmatrix}, \tag{55d}$$

$$\mathbf{\Psi}_{e/e,J} = \begin{bmatrix} \boldsymbol{\psi}_{e/e}(\mathbf{r}_{1,1}) & \cdots & \boldsymbol{\psi}_{e/e}(\mathbf{r}_{1,j}) & \cdots & \boldsymbol{\psi}_{e/e}(\mathbf{r}_{1,J}), \end{bmatrix} \tag{56a}$$

$$\mathbf{\Psi}_{e/o,J} = \begin{bmatrix} \boldsymbol{\psi}_{e/o}(\mathbf{r}_{1,1}) & \cdots & \boldsymbol{\psi}_{e/o}(\mathbf{r}_{1,j}) & \cdots & \boldsymbol{\psi}_{e/o}(\mathbf{r}_{1,J}) \end{bmatrix}, \tag{56b}$$

$$\mathbf{\Psi}_{o/e,J} = \begin{bmatrix} \boldsymbol{\psi}_{o/e}(\mathbf{r}_{1,1}) & \cdots & \boldsymbol{\psi}_{o/e}(\mathbf{r}_{1,j}) & \cdots & \boldsymbol{\psi}_{o/e}(\mathbf{r}_{1,J}) \end{bmatrix}, \tag{56c}$$

$$\mathbf{\Psi}_{o/o,J} = \begin{bmatrix} \boldsymbol{\psi}_{o/o}(\mathbf{r}_{1,1}) & \cdots & \boldsymbol{\psi}_{o/o}(\mathbf{r}_{1,j}) & \cdots & \boldsymbol{\psi}_{o/o}(\mathbf{r}_{1,J}) \end{bmatrix}, \tag{56d}$$

$$\tilde{\mathbf{f}}_{e/e}(\omega) = \begin{bmatrix} f_{e/e,1}(\omega) & \cdots & f_{e/e,j}(\omega) & \cdots & f_{e/e,J}(\omega) \end{bmatrix}^{\mathrm{T}}, \tag{57a}$$

$$\tilde{\mathbf{f}}_{e/o}(\omega) = \begin{bmatrix} f_{e/o,1}(\omega) & \cdots & f_{e/o,j}(\omega) & \cdots & f_{e/o,J}(\omega) \end{bmatrix}^{\mathrm{T}}, \tag{57b}$$

$$\tilde{\mathbf{f}}_{o/e}(\omega) = \begin{bmatrix} f_{o/e,1}(\omega) & \cdots & f_{o/e,j}(\omega) & \cdots & f_{o/e,J}(\omega) \end{bmatrix}^{\mathrm{T}}, \tag{57c}$$

$$\tilde{\mathbf{f}}_{o/o}(\omega) = \begin{bmatrix} f_{o/o,1}(\omega) & \cdots & f_{o/o,j}(\omega) & \cdots & f_{o/o,J}(\omega) \end{bmatrix}^{\mathrm{T}}, \tag{57d}$$

$$\begin{bmatrix} f_{e/e,j}(\omega) \\ f_{e/o,j}(\omega) \\ f_{o/e,j}(\omega) \\ f_{o/o,j}(\omega) \end{bmatrix} = \begin{bmatrix} +1 & +1 & +1 & +1 \\ +1 & +1 & -1 & -1 \\ +1 & -1 & -1 & +1 \\ +1 & -1 & +1 & -1 \end{bmatrix} \begin{bmatrix} f_{1,j}(\omega) \\ f_{2,j}(\omega) \\ f_{3,j}(\omega) \\ f_{4,j}(\omega) \end{bmatrix} \quad (j = 1, 2, \ldots, J), \tag{58}$$

$$\mathbf{r}_{1,i} = (x_{1,i}, y_{1,i}), \quad \mathbf{r}_{2,i} = (L_x - x_{1,i}, y_{1,i}), \quad \mathbf{r}_{3,i} = (L_x - x_{1,i}, L_y - y_{1,i}), \quad \mathbf{r}_{4,i} = (x_{1,i}, L_y - y_{1,i}), \tag{59}$$

$$\mathbf{r}_{1,j} = (x_{1,j}, y_{1,j}), \quad \mathbf{r}_{2,j} = (L_x - x_{1,j}, y_{1,j}), \quad \mathbf{r}_{3,j} = (L_x - x_{1,j}, L_y - y_{1,j}), \quad \mathbf{r}_{4,j} = (x_{1,j}, L_y - y_{1,j}), \tag{60}$$

$$\mathbf{Y}_{e/e}(\omega) = \mathrm{diag}\begin{bmatrix} Y_{1/1} & \cdots & Y_{n_{x,o}/n_{y,o}} & \cdots & Y_{N_{x,o}/N_{y,o}} \end{bmatrix}, \tag{61a}$$

$$\mathbf{Y}_{e/o}(\omega) = \mathrm{diag}\begin{bmatrix} Y_{1/2} & \cdots & Y_{n_{x,o}/n_{y,e}} & \cdots & Y_{N_{x,o}/N_{y,e}} \end{bmatrix}, \tag{61b}$$

$$\mathbf{Y}_{o/e}(\omega) = \mathrm{diag}\begin{bmatrix} Y_{2/1} & \cdots & Y_{n_{x,e}/n_{y,o}} & \cdots & Y_{N_{x,e}/N_{y,o}} \end{bmatrix}, \tag{61c}$$

$$\mathbf{Y}_{o/o}(\omega) = \mathrm{diag}\begin{bmatrix} Y_{2/2} & \cdots & Y_{n_{x,e}/n_{y,e}} & \cdots & Y_{N_{x,e}/N_{y,e}} \end{bmatrix}, \tag{61d}$$

$$\omega_n = \omega_{n_x/n_y} = \sqrt{\frac{D}{\rho_s h}} \left\{ \left(\frac{n_x \pi}{L_x}\right)^2 + \left(\frac{n_y \pi}{L_y}\right)^2 \right\}, \tag{62}$$

$$D = \frac{Eh^3}{12(1 - v^2)}, \tag{63}$$

where E the Young's modulus of the plate, ρ_s the density of the plate, v the Poisson ratio of the plate, h is the thickness of the plate, η_n the modal loss factor of the nth structural mode. Since Eq. (50) is the Hermitian quadratic form of the complex control force vector [1], the optimum set of the control forces, which uniquely produce the global minimum value of the quadratic function, is given by

$$\begin{bmatrix} \tilde{\mathbf{f}}_{e/e}(\omega) \\ \tilde{\mathbf{f}}_{e/o}(\omega) \\ \tilde{\mathbf{f}}_{o/e}(\omega) \\ \tilde{\mathbf{f}}_{o/o}(\omega) \end{bmatrix} = - \begin{bmatrix} \{\mathbf{A}^{\mathrm{H}}_{e/e}(\omega)\mathbf{A}_{e/e}(\omega)\}^{-1}\mathbf{A}^{\mathrm{H}}_{e/e}(\omega)\mathbf{b}_{e/e}(\omega) \\ \{\mathbf{A}^{\mathrm{H}}_{e/o}(\omega)\mathbf{A}_{e/o}(\omega)\}^{-1}\mathbf{A}^{\mathrm{H}}_{e/o}(\omega)\mathbf{b}_{e/o}(\omega) \\ \{\mathbf{A}^{\mathrm{H}}_{o/e}(\omega)\mathbf{A}_{o/e}(\omega)\}^{-1}\mathbf{A}^{\mathrm{H}}_{o/e}(\omega)\mathbf{b}_{o/e}(\omega) \\ \{\mathbf{A}^{\mathrm{H}}_{o/o}(\omega)\mathbf{A}_{o/o}(\omega)\}^{-1}\mathbf{A}^{\mathrm{H}}_{o/o}(\omega)\mathbf{b}_{o/o}(\omega) \end{bmatrix}. \tag{64}$$

From Ref. [19], upper bounds on the radiation efficiencies of the individual radiation clusters of a rectangular plate at low nondimensional frequencies, $kL_y < kL_x \ll 1$, are defined as

$$\sigma_{\max,e/e} \approx \frac{\pi}{2}\left(\frac{L_y}{L_x}\right)\left(\frac{kL_x}{\pi}\right)^2, \tag{65a}$$

$$\sigma_{\max,e/o} \approx \frac{\pi^3}{72}\left(\frac{L_y}{L_x}\right)^3\left(\frac{kL_x}{\pi}\right)^4, \tag{65b}$$

$$\sigma_{\max,o/e} \approx \frac{\pi^3}{72}\left(\frac{L_y}{L_x}\right)\left(\frac{kL_x}{\pi}\right)^4, \tag{65c}$$

$$\sigma_{\max,o/o} \approx \frac{\pi}{4320}\left(\frac{L_y}{L_x}\right)^3\left(\frac{kL_x}{\pi}\right)^6. \tag{65d}$$

From Eq. (65), the even/even radiation cluster proves to be much more efficient contributor than the other radiation clusters, because it has the less order dependence in the exponent on the nondimensional frequency with $kL_x \ll 1$. The even/even radiation cluster has a second-order dependence on kL_x, while the even/odd radiation cluster has a fourth-order dependence on kL_x, the odd/even radiation cluster has a fourth-order dependence on kL_x, and the odd/odd radiation cluster has a sixth-order dependence on kL_x. In contrast, at high frequencies upper bounds on the radiation efficiencies of the individual radiation clusters may be comparable to each other. This allows one to get an insight into reasonable strategies for the active control of the sound transmission: for low nondimensional frequency excitation the even/even radiation cluster, which has much higher radiation efficiency than the other radiation clusters, should be preferentially measured and controlled; and for high nondimensional frequency excitation all radiation clusters, which have comparable radiation efficiencies to each other, should be parallel measured and controlled. Note again that radiation cluster control can parallel measure and control the designated radiation clusters without causing observation spillover as well as control spillover among the radiation clusters.

3.2. Numerical simulations: radiation cluster control versus conventional active vibration control, radiation modal control, and volume velocity cancellation

In this section, the active control of the sound transmission in the case of the simply supported rectangular plate shown in Fig. 2 is simulated to verify the validity of radiation cluster control presented in the work. To compare the control performance of radiation cluster control with those of traditional control methods, conventional active vibration control, radiation modal control, and volume velocity cancellation are also conducted. In all the control methods, 100 velocity measurements at symmetric coordinates and all or one of the 4 control forces at symmetric coordinates are used, as shown in Fig. 3 and Table 1. Though the number and location of both the velocity measurements and control forces have a significant effect upon the control

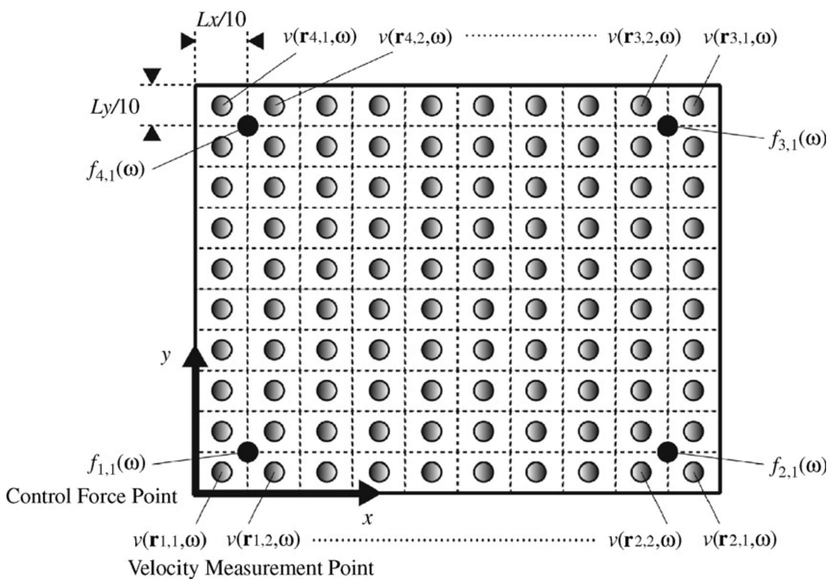

Fig. 3. A rectangular plate with locations of sensors and actuators.

Table 1
Configuration of the velocity measurements and control forces in each control method

Control method	Velocity measurement	Control force	Input/output
Radiation cluster	All the 100 points	$f_{1,1}(\omega)$, $f_{2,1}(\omega)$, $f_{3,1}(\omega)$, $f_{4,1}(\omega)$	1/25
Structural mode	All the 100 points	$f_{1,1}(\omega)$	1/100
Radiation mode	All the 100 points	$f_{1,1}(\omega)$, $f_{2,1}(\omega)$, $f_{3,1}(\omega)$, $f_{4,1}(\omega)$	4/100
Volume velocity	All the 100 points	$f_{1,1}(\omega)$, $f_{2,1}(\omega)$, $f_{3,1}(\omega)$, $f_{4,1}(\omega)$	1/1

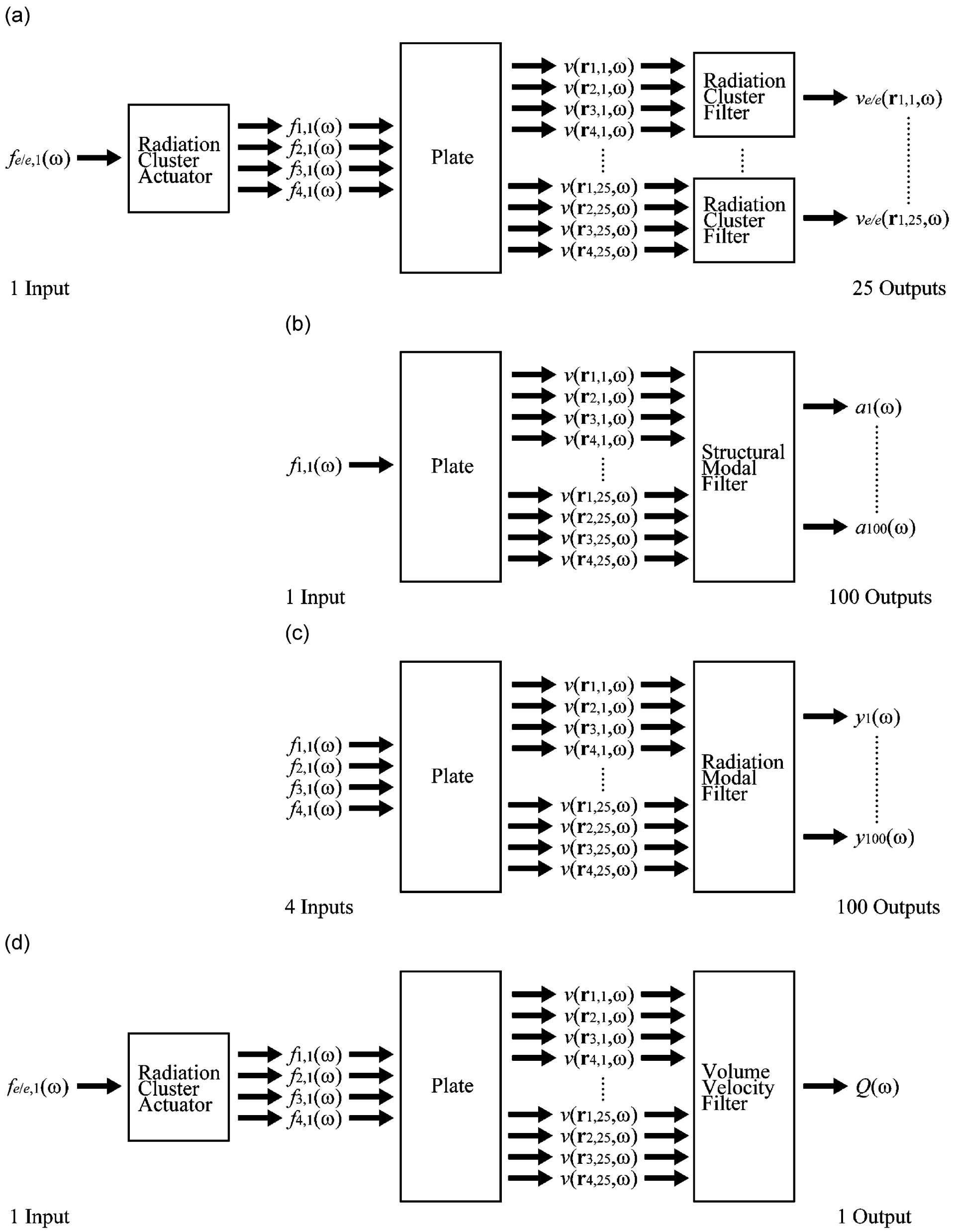

Fig. 4. Signal flow of each control method: (a) Radiation cluster control. (b) Structural modal control. (c) Radiation modal control. (d) Volume velocity cancellation.

performance, the number and location in this simulation are not specially optimized because such a problem is not the main issue in this paper.

In the case of radiation cluster control, 25 sets of the radiation cluster filters and 1 set of the radiation cluster actuator are built for a single radiation cluster, as illustrated in Fig. 4(a). This arrangement is 1 input 25 outputs, i.e., single input multiple outputs (SIMO). The sum of the 25 squared complex normal velocities of a single radiation cluster is minimized in accordance with Eq. (64). If all the radiation clusters are controlled at the same time, the arrangement is 4-parallel-SIMO.

In the case of conventional vibration control, i.e., structural modal control, 100 sets of the structural modal filters [11] are built, and one of the 4 control forces, i.e., the point control force at ($L_x/10$, $L_y/10$), is used, as illustrated in Fig. 4(b). Note that the structural modal filters in this simulation provide the estimates with high precision because the number of the measurement points equals the number of the structural modes of interest, thus the performance of structural modal control is not deteriorated due to the estimation errors. This arrangement is 1 input 100 outputs, i.e., SIMO. The sum of the 100 squared complex amplitudes of the structural modes is minimized by conventional feedforward quadratic optimization in the same manner as radiation cluster control.

In the case of radiation modal control, 100 sets of the radiation modal filters [3,5–8] are built, and all the 4 control forces are used, as illustrated in Fig. 4(c). This arrangement is 4 input 100 outputs, i.e., MIMO. The sum of the 100 squared complex amplitudes of the radiation modes is minimized by conventional feedforward quadratic optimization in the same manner as the above control methods.

In the case of volume velocity cancellation, a volume velocity filter, which sums the complex velocities of the elemental radiators multiplied by the elemental areas in accordance with Eq. (12), and 1 set of the radiation cluster actuator for the even/even radiation cluster are built, as illustrated in Fig. 4(d). This arrangement is 1 input 1 output, i.e., SISO. The squared volume velocity is minimized by conventional feedforward quadratic optimization in the same manner as the above control methods.

The dimensions of the plate are $L_x = 0.38\,\text{m}$, $L_y = 0.30\,\text{m}$, and $h = 2\,\text{mm}$, the Young's modulus of the plate is $E = 71\,\text{GPa}$, the density of the plate is $\rho_s = 2720\,\text{kg/m}^3$, the Poisson ratio of the plate is $v = 0.33$, and the modal loss factor of the structural modes are uniformly $\eta_n = 0.001$. Sound speed in the air is $c_0 = 343$ m/s, and the density of the air is $\rho_0 = 1.21\,\text{kg/m}^3$. The nondimensional frequency, $kL_x = 1$, corresponds to 143.7 Hz. An external acoustic field is assumed to excite the plate, which, in turn, radiates sound into the opposite side of the

Table 2
Natural frequency and radiation cluster attribute of the structural modes of the plate

Modal index	Natural freq. (Hz)	Cluster attribute
1/1	44	Even/even
2/1	95	Odd/even
1/2	126	Even/odd
2/2	177	Odd/odd
3/1	180	Even/even
1/3	262	Even/even
3/2	262	Even/odd
4/1	299	Odd/even
2/3	313	Odd/even
4/2	381	Odd/odd
3/3	398	Even/even
5/1	452	Even/even
1/4	453	Even/odd
2/4	504	Odd/odd
4/3	517	Odd/even
5/2	534	Even/odd
3/4	589	Even/odd
6/1	639	Odd/even
5/3	670	Even/even
1/5	698	Even/even

plate. A harmonic plane wave incident on the plate at the elevation angle from the horizontal, $\theta = \pi/4$, and the azimuth angle from the x axis, $\varphi = \pi/4$, will create a pressure field, $p_i(\mathbf{r},\omega)$, in the plane of the plate given by [14]

$$p_i(\mathbf{r},\omega) = P_i e^{-j(k_x x + k_y y)}, \tag{66}$$

where $k_x = k \sin\theta \cos\varphi$ is the wavenumber in the x direction, and $k_y = k \sin\theta \sin\varphi$ is the wavenumber in the y direction. The numbers of structural modes to be considered in the simulation are $N_x = 10$ and $N_y = 10$. Table 2 presents a list of the natural frequencies of the plate. Note that many of the results quoted below will be expressed in terms of a power transmission ratio [14]. This is defined as the acoustic power radiated from the plate divided by the acoustic power incident on the plate if the plate were rigid. The power incident on the

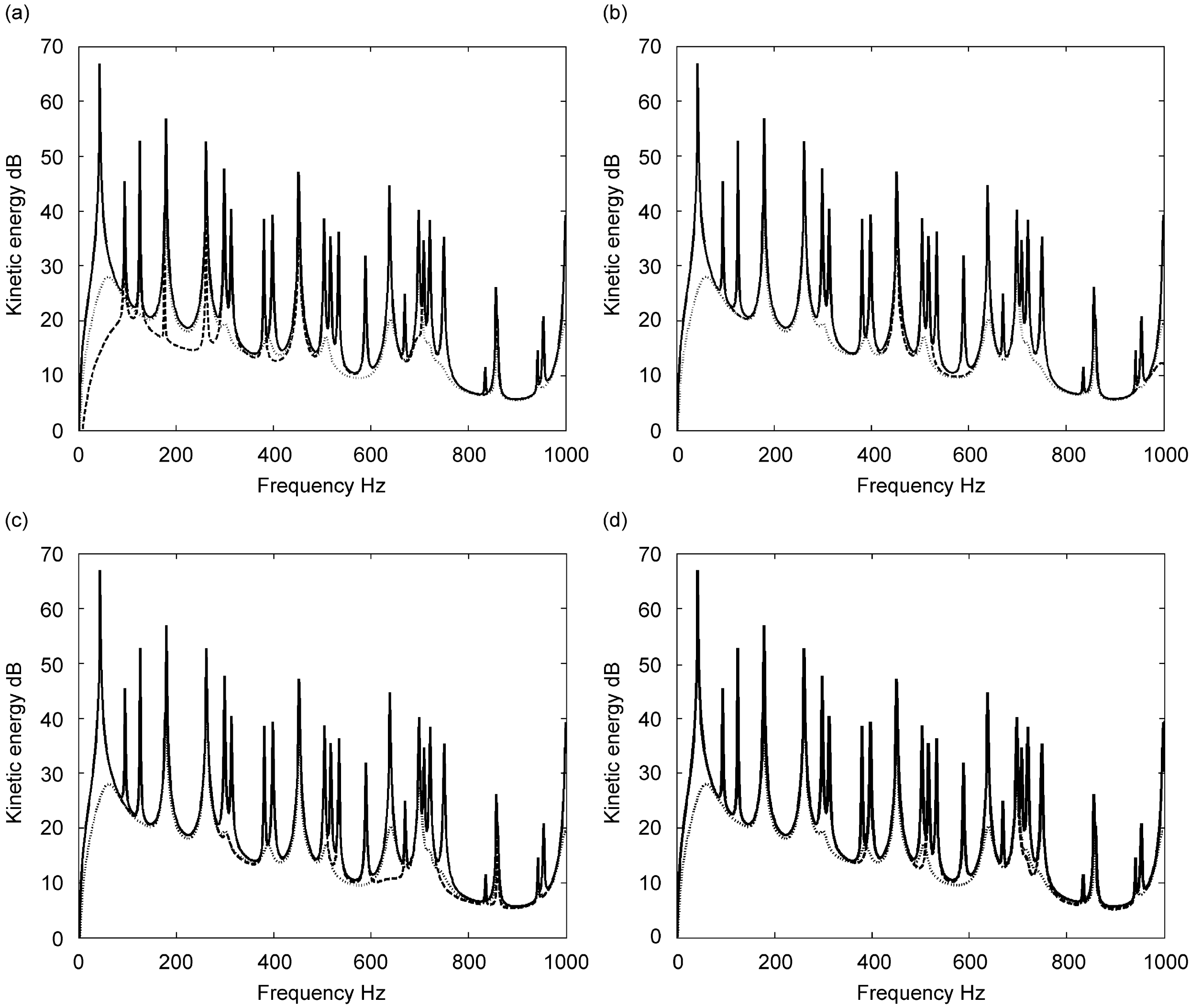

Fig. 5. Kinetic energy of the plate before and after radiation cluster control with the error criterion being a specific radiation cluster (dashed) and structural modal control (dotted): (a) Kinetic energy of the plate before (solid) and after radiation cluster control with the error criterion being the even/even radiation cluster (dashed) and structural modal control (dotted). (b) Kinetic energy of the plate before (solid) and after radiation cluster control with the error criterion being the even/odd radiation cluster (dashed) and structural modal control (dotted). (c) Kinetic energy of the plate before (solid) and after radiation cluster control with the error criterion being the odd/even radiation cluster (dashed) and structural modal control (dotted). (d) Kinetic energy of the plate before (solid) and after radiation cluster control with the error criterion being the odd/odd radiation cluster (dashed) and structural modal control (dotted).

plate area if it were rigid, W_i, is written as

$$W_i = \frac{|P_i|^2 L_x L_y}{2\rho_0 c_0} \cos\theta. \quad (67)$$

The sound transmission ratio, $T(\omega)$, is then written as

$$T(\omega) = \frac{W(\omega)}{W_i}, \quad (68)$$

where $T(\omega)$ is the inverse of the transmission loss, and is used here as a convenient normalization for the radiated acoustic power.

Figs. 5 and 6 present the kinetic energy and sound transmission ratio of the plate before and after radiation cluster control with the error criterion being the sum of the squared complex normal velocities of the

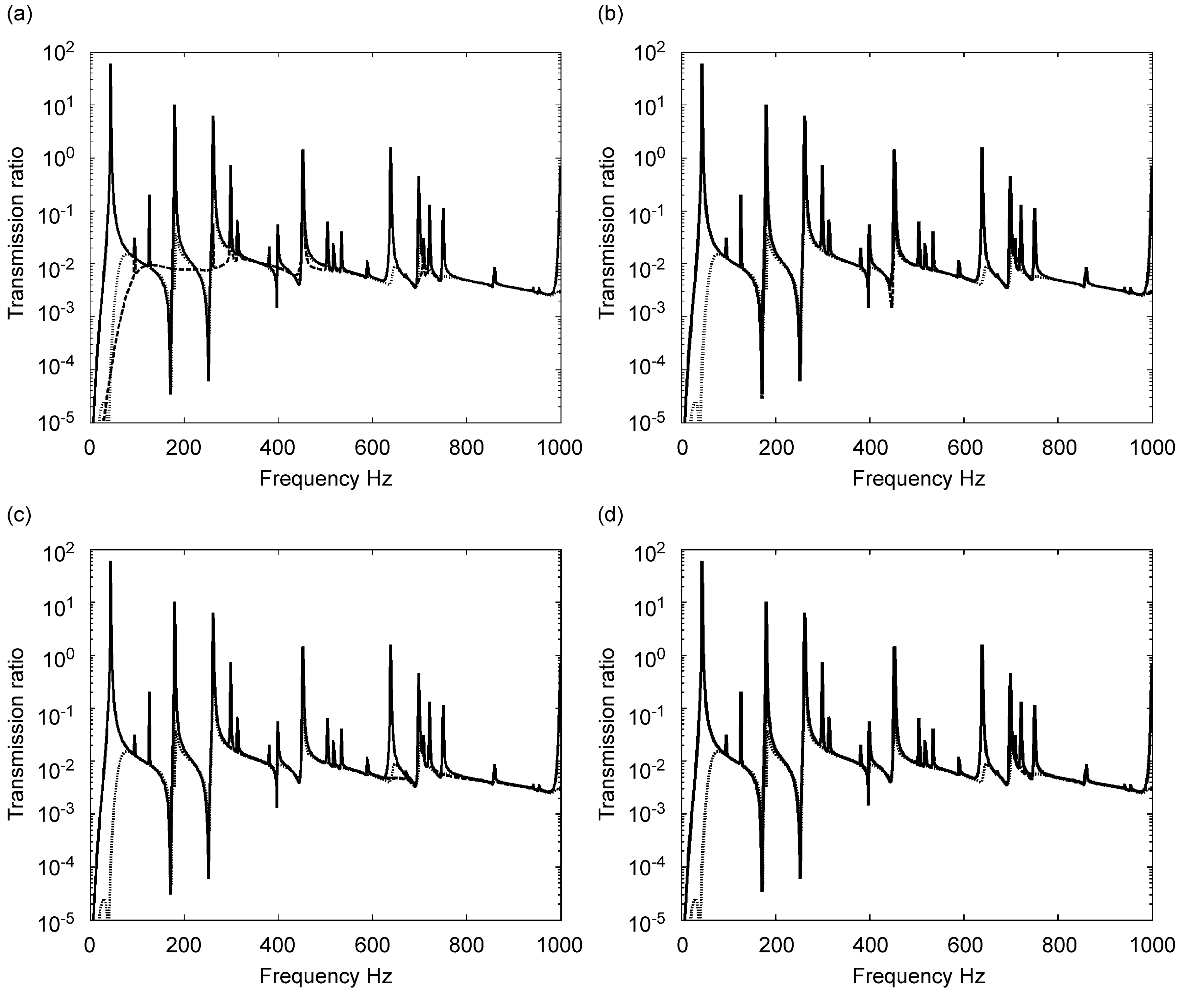

Fig. 6. Sound transmission ratio of the plate before and after radiation cluster control with the error criterion being a specific radiation cluster (dashed) and structural modal control (dotted): (a) Sound transmission ratio of the plate before (solid) and after radiation cluster control with the error criterion being the even/even radiation cluster (dashed) and structural modal control (dotted). (b) Sound transmission ratio of the plate before (solid) and after radiation cluster control with the error criterion being the even/odd radiation cluster (dashed) and structural modal control (dotted). (c) Sound transmission ratio of the plate before (solid) and after radiation cluster control with the error criterion being the odd/even radiation cluster (dashed) and structural modal control (dotted). (d) Sound transmission ratio of the plate before (solid) and after radiation cluster control with the error criterion being the odd/odd radiation cluster (dashed) and structural modal control (dotted).

individual radiation clusters and structural modal control. The following are clear from Fig. 5: radiation cluster control independently reduces the kinetic energy which the designated radiation cluster contributes; and structural modal control reduces the kinetic energy which all structural modes contribute. Note that the reduction of the kinetic energy which each of the radiation clusters contributes by radiation cluster control with the error criterion being the associated radiation cluster is greater than that by structural modal control. The observed behavior can be explained by taking into consideration that radiation cluster control can independently measure and control the designated radiation cluster without causing spillover among the radiation clusters, while structural modal control measures and controls all structural modes with causing spillover among the radiation clusters. It is possible in structural modal control that a set of the structural modes which contribute the kinetic energy are excited out of phase with another set of the structural modes which also contribute the kinetic energy such that their contributions largely cancel each other. Under these circumstances, structural modal control cannot decrease one of the sets of the structural modes because it

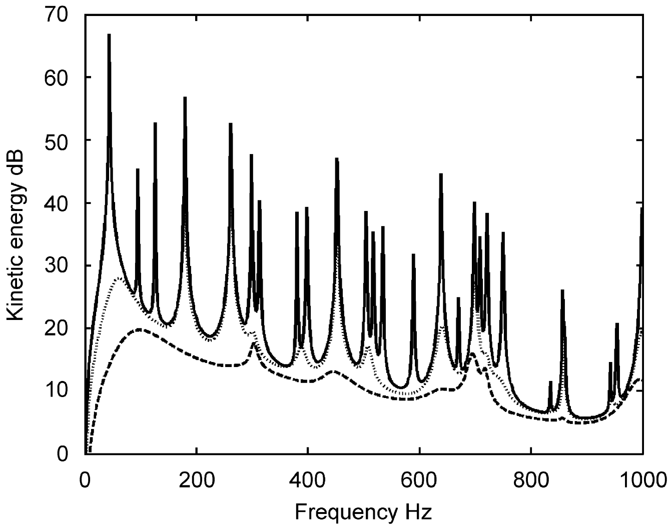

Fig. 7. Kinetic energy of the plate before and after radiation cluster control with the error criterion being all the radiation clusters (dashed) and structural modal control (dotted).

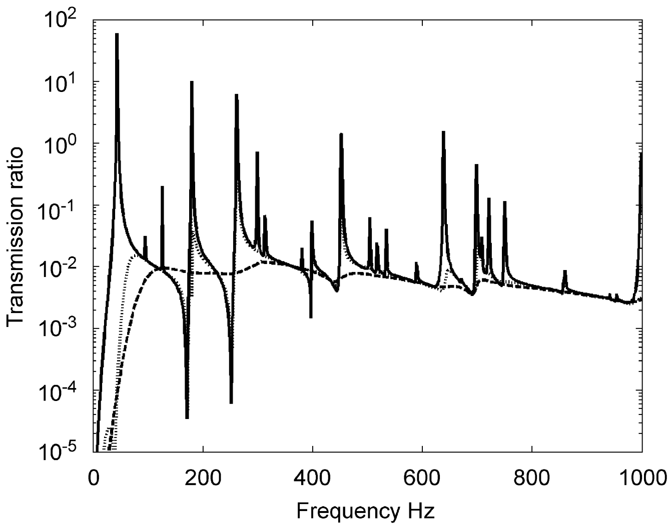

Fig. 8. Sound transmission ratio of the plate before and after radiation cluster control with the error criterion being all the radiation clusters (dashed) and structural modal control (dotted).

causes increasing the other set of the structural modes. On the other hand, radiation cluster control may overcome such a problem in the cluster sense, thereby decreasing the designated radiation cluster. It is clear from Figs. 5 and 6 that at low nondimensional frequencies the radiation efficiency of the even/even radiation cluster is much higher than those of the other radiation clusters, and at high nondimensional frequencies the radiation efficiencies of all the radiation clusters are comparable to each other, as expected. This implies that for low nondimensional frequency excitation minimizing the even/even radiation cluster may be effective for reducing the sound transmission, and for high nondimensional frequency excitation minimizing all the radiation clusters may be effective for reducing the sound transmission. Fig. 6 shows that at low nondimensional frequencies radiation cluster control with the error criterion being the even/even radiation cluster achieves the greater reduction of the sound transmission ratio than structural modal control, and at high nondimensional frequencies radiation cluster control with the error criterion being any single radiation cluster achieves the less reduction of the sound transmission ratio than structural modal control, as expected.

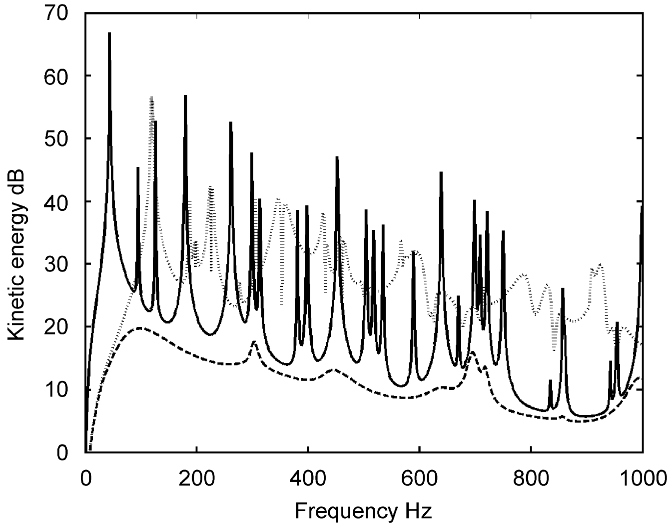

Fig. 9. Kinetic energy of the plate before and after radiation cluster control with the error criterion being all the radiation clusters (dashed) and radiation modal control (dotted).

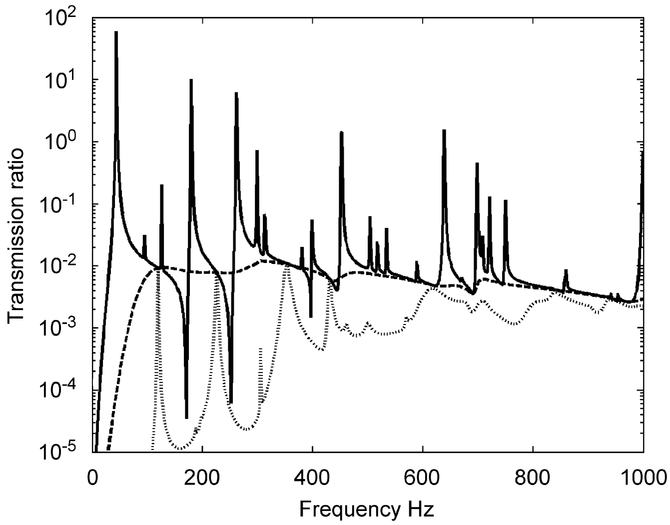

Fig. 10. Sound transmission ratio of the plate before and after radiation cluster control with the error criterion being all the radiation clusters (dashed) and radiation modal control (dotted).

Figs. 7 and 8 present the kinetic energy and sound transmission ratio of the plate before and after radiation cluster control with the error criterion being all the sum of the squared complex normal velocities of the individual radiation clusters, i.e., a 4-parallel-SIMO arrangement of radiation cluster control, and structural modal control. It is clear from Figs. 7 and 8 that for the entire range of frequencies under consideration radiation cluster control achieves the greater reduction of both the kinetic energy and the sound transmission ratio than structural modal control. It should be noted that if the 4 control forces are used in structural modal control, the performance of structural modal control would agree with those of 4-parallel-SIMO radiation cluster control. However, the arrangement of structural modal control is then 4 inputs 100 outputs, i.e., MIMO, and it is much more complicate than radiation cluster control.

Figs. 9 and 10 present the kinetic energy and sound transmission ratio of the plate before and after radiation cluster control with the error criterion being all the sum of the squared complex normal velocities of the individual radiation clusters and radiation modal control. It is clear from Figs. 9 and 10 that for the

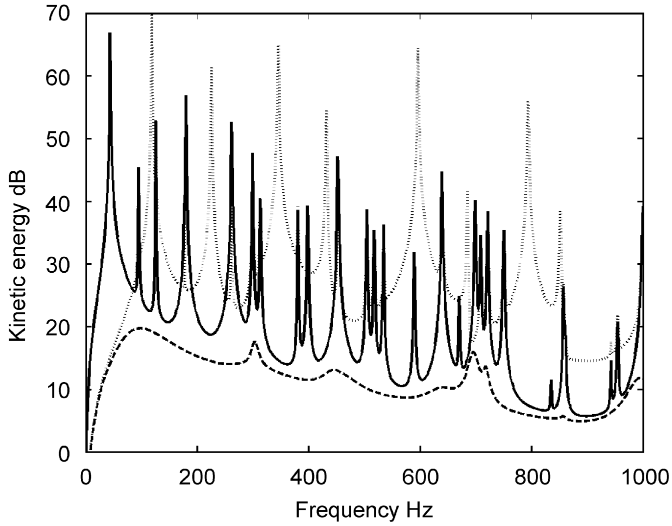

Fig. 11. Kinetic energy of the plate before and after radiation cluster control with the error criterion being all the radiation clusters (dashed) and volume velocity cancellation (dotted).

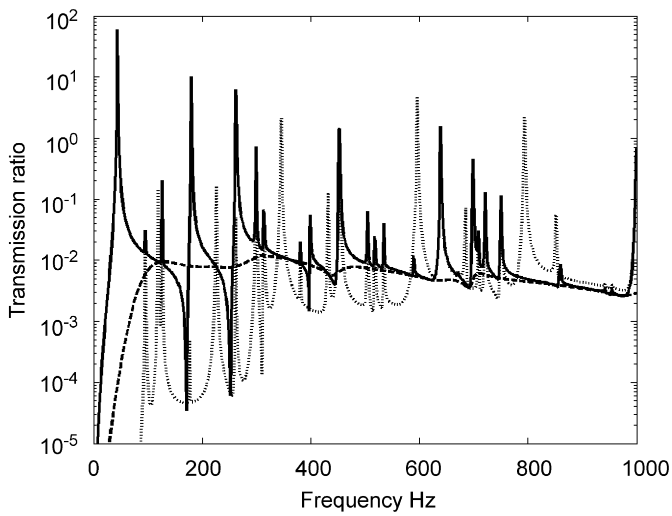

Fig. 12. Sound transmission ratio of the plate before and after radiation cluster control with the error criterion being all the radiation clusters (dashed) and volume velocity cancellation (dotted).

entire range of frequencies under consideration radiation cluster control achieves the greater reduction of the kinetic energy than radiation modal control, whereas for the entire range of frequencies under consideration radiation cluster control achieves the less reduction of the sound transmission ratio than radiation modal control. Note again that radiation modal control is an ideal strategy for the active control of the sound transmission, but it may be difficult to implement due to the complexity of the radiation modal filters.

Figs. 11 and 12 present the kinetic energy and sound transmission ratio of the plate before and after radiation cluster control with the error criterion being all the sum of the squared complex normal velocities of the individual radiation clusters and volume velocity cancellation. It is clear from Fig. 11 that for the entire range of frequencies under consideration radiation cluster control achieves the greater reduction of the kinetic energy than volume velocity cancellation. The observed behavior can be explained by taking into consideration that radiation cluster control parallel controls all radiation clusters, whereas volume velocity cancellation controls only the even/even radiation cluster because volume velocity cancellation results in a special case of radiation cluster control with the error criterion being the even/even radiation cluster. Additionally, it should be noted that volume velocity cancellation does not derive the velocity of the plate to zero at any point but derives its average velocity to zero, and therefore the kinetic energy is not necessarily decreased and can be increased. It is clear from Fig. 12 that at low nondimensional frequencies radiation cluster control achieves the less reduction of the sound transmission ratio than volume velocity cancellation, whereas at high nondimensional frequencies radiation cluster control achieves the greater reduction of the sound transmission than volume velocity cancellation. The observed behavior can be explained by taking into consideration that at low nondimensional frequencies the complex volume velocity is a good approximation of the amplitude of the lowest-order radiation mode which at low nondimensional frequencies accounts for the majority of the radiated acoustic power, whereas at high nondimensional frequencies the majority of the acoustic power is not only the complex volume velocity, i.e., the even/even radiation cluster, but also the other radiation clusters. From a viewpoint of the reduction of the sound transmission ratio for the entire range of frequencies under consideration, radiation cluster control is better than volume velocity cancellation.

4. Conclusions

For the purpose of controlling sound transmission through a symmetric structure into free space based upon structural error sensing, "radiation clusters" which are the orthogonal contributors with respect to the radiated acoustic field have been derived. The methodology for filtering the individual radiation clusters with sets of point sensors, termed "radiation cluster filters", as well as the methodology for actuating the individual radiation clusters with sets of point forces, termed "radiation cluster actuators", have been developed. Radiation cluster filters and actuators can be built via simple arithmetic process such as addition and subtraction without the knowledge of the structural modal functions, the acoustic impedance of each pair of the discrete sensor locations, and the radiation resistance of each pair of the structural modes. This allows one to implement the radiation cluster filters and actuators in practice. By combining the radiation cluster filters and actuators, "radiation cluster control" which can independently measure and control the designated radiation cluster without causing observation spillover and control spillover is performed. Examples of radiation cluster control of a simply supported rectangular plate in an infinite baffle have been presented. Four radiation clusters are defined in the plate model. At low nondimensional frequencies (excitation frequencies for which the size of the plate is small compared with the acoustic wave length), the radiation efficiency of a specific radiation cluster is significant. The most significantly influential radiation cluster consists of the structural modes associated with the volumetric components, as expected. At high nondimensional frequencies, the radiation efficiencies of all the radiation clusters are comparable to each other. It has been demonstrated that for low nondimensional frequency excitation independently minimizing the squared complex normal velocities of the most influential radiation cluster results in a significant attenuation of the sound transmission, and for high nondimensional frequency excitation parallel minimizing the squared complex normal velocities of all the four radiation clusters results in a significant attenuation of the sound transmission.

References

[1] S.D. Snyder, C.H. Hansen, Mechanisms of active noise control by vibration sources, *Journal of Sound and Vibration* 147 (1991) 519–525.

[2] J. Pan, S.D. Snyder, C.H. Hansen, C.R. Fuller, Active control of far-field sound radiated by a rectangular panel: a general analysis, *Journal of the Acoustical Society of America* 91 (1992) 2056–2066.

[3] S.J. Elliott, M.E. Johnson, Radiation modes and the active control of sound power, *Journal of the Acoustical Society of America* 94 (1993) 2194–2204.

[4] G.V. Borgiotti, The power radiated by a vibration body in an acoustic fluid and its determination from boundary measurements, *Journal of the Acoustical Society of America* 88 (1990) 1884–1893.

[5] G.P. Gibbs, R.L. Clark, D.E. Cox, J.S. Vipperman, Radiation modal expansion: application to active structural acoustic control, *Journal of the Acoustical Society of America* 107 (2000) 332–339.

[6] A.P. Berkhoff, Piezoelectric sensor configuration for active structural acoustic control, *Journal of Sound and Vibration* 246 (2001) 175–183.

[7] A.P. Berkhoff, Broadband radiation modes: estimation and active control, *Journal of the Acoustical Society of America* 111 (2002) 1295–1305.

[8] T. Chanpheng, H. Yamada, T. Miyata, H. Katsuchi, Application of radiation modes to the problem of low-frequency noise from a highway bridge, *Applied Acoustics* 65 (2004) 109–123.

[9] S.D. Snyder, N. Tanaka, On feedforward active control of sound and vibration using vibration error signals, *Journal of the Acoustical Society of America* 94 (1993) 2181–2193.

[10] B.S. Cazzolato, C.H. Hansen, Active control of sound transmission using structural error sensing, *Journal of the Acoustical Society of America* 104 (1998) 2878–2889.

[11] D.R. Morgan, An adaptive modal-based active control system, *Journal of the Acoustical Society of America* 89 (1991) 248–256.

[12] R.L. Clark, S.E. Burke, Practical limitations in achieving shaped modal sensors with induced strain materials, *Journal of Vibration and Acoustics* 118 (1996) 668–675.

[13] N. Tanaka, Y. Kikushima, N.J. Fergusson, One-dimensional distributed modal sensors and the active modal control for planar structures, *Journal of Acoustical Society of America* 104 (1998) 217–225.

[14] M.E. Johnson, S.J. Elliott, Active control of sound radiation using volume velocity cancellation, *Journal of the Acoustical Society of America* 98 (1995) 2174–2186.

[15] M.E. Johnson, S.J. Elliott, Active control of sound radiation from vibrating surfaces using arrays of discrete actuators, *Journal of Sound and Vibration* 207 (1997) 743–759.

[16] X. Pan, T.J. Sutton, S.J. Elliott, Active control of sound transmission through a double-leaf partition by volume velocity cancellation, *Journal of the Acoustical Society of America* 104 (1998) 2828–2835.

[17] J.-C. Lee, J.-C. Chen, Active control of sound radiation from a rectangular plate excited by a line moment, *Journal of Sound and Vibration* 220 (1999) 99–115.

[18] C. Maury, P. Gardonio, S.J. Elliott, Active control of the flow-induced noise transmitted through a panel, *AIAA Journal* 39 (2001) 1860–1867.

[19] P. Gardonio, Y.S. Lee, S.J. Elliott, Analysis and measurement of a matched volume velocity sensor and uniform force actuator for active structural acoustic control, *Journal of the Acoustical Society of America* 110 (2001) 3025–3031.

[20] T.C. Sors, S.J. Elliott, Volume velocity estimation with accelerometer arrays for active structural acoustic control, *Journal of Sound and Vibration* 258 (2002) 867–883.

[21] K. Henrioulle, P. Sas, Experimental validation of a collocated PVDF volume velocity sensor/actuator pair, *Journal of Sound and Vibration* 265 (2003) 489–506.

[22] K.A. Cunefare, G.H. Koopmann, The minimum multimodal radiation efficiency of baffled finite beams, *Journal of the Acoustical Society of America* 90 (1991) 2521–2529.

[23] M.N. Currey, K.A. Cunefare, The radiation modes of baffled finite plates, *Journal of the Acoustical Society of America* 98 (1995) 1570–1580.

[24] K.A. Cunefare, M.N. Currey, M.E. Johnson, S.J. Elliott, The radiation efficiency grouping of free-space acoustic radiation modes, *Journal of the Acoustical Society of America* 109 (2001) 203–215.

[25] T. Kaizuka, N. Tanaka, Radiation clusters and the active control of sound transmission into a symmetric enclosure, *Journal of the Acoustical Society of America* 121 (2007) 922–937.